GLOBAL ENVIRONMENTAL MODELLING SYSTEMS

Perth Office	Melbourne Office	Queensland Office
Scott Langtry	Graeme Hubbert, Steve Oliver	Brian King
PO Box 102	PO Box 149	PO Box 1679
Bassendean WA 6054	Warrandyte Vic. 3113	Surfers Paradise Qld 4217
TEL: +61 (0)8 9379 8946	TEL: +61 (0)3 9712 0016	Tel: +61 (0)7 5592 5331
FAX: +61 (0)8 9379 8947	FAX: +61 (0)3 9712 0017	Fax: +61 (0)7 5527 1162
MOB: +61 (0)418 827 754	Mob: +61 (0)418 36 63 36	Mob: +61 (0)419 763 060
scottl@gems-aus.com	gdh@gems-aus.com	Oilmap@ozemail.com.au

GOLD COAST BROADWATER STUDY

Storm Tide Return Periods

and

1974 Floodwater Modelling

for

Gold Coast City Council

by

Kathleen McInnes[1], Graeme Hubbert[2], Steve Oliver[2], and Debbie Abbs[1]

CSIRO

Atmospheric Research

May 2000

1 CSIRO Atmospheric Research
2 Global Environmental Modelling Systems

Executive Summary **3**
Disclaimer **5**
1. Introduction **6**
2. Extreme Events and Coastal Impacts **7**
2.1 Coastal Effects 7
2.2 Meteorology 8
3. Models **9**
3.1 Storm Surge Model 9
3.2 Wave Model 11
3.3 Atmospheric Fields 11
3.3.1 Cyclone Model 12
3.3.2 NCEP Analyses 12
3.3.3 Regional Atmospheric Modelling System (RAMS) 12
4. Methodology for Evaluating Storm tide Statistics **13**
4.1 Near-shore and Coast-Crossing Tropical Cyclones 13
4.1.1 Cyclone Intensity 13
4.1.2 Cyclone Tracks 15
4.1.3 Modelling the Storm tides 16
4.2 Offshore Tropical Cyclones and East Coast Lows 17
4.2.1 Selection of Atmospheric Conditions 17
4.2.2 Modelling the Storm tides 18
4.3 Event Probability: Return Periods of Sea Level 18
5. Results **19**
5.1 Coastal-Crossing Cyclones 19
5.2 Offshore Tropical Cyclones and East Coast Lows 20
5.3 Combined Sea-Level Predictions 22
5.4 Discussion 22
5.5 Uncertainty Estimates 23
5.6 Comparison with Earlier Studies 23
6. Case Studies **24**
6.1 Case 1: 25 April 1989 24
6.1.1 Atmospheric Model Results 24
6.1.2 Tidal Model Results 26
6.1.3 Wave Model Results 27
6.1.4 Storm Surge and Wave Setup Results 28
6.2 Case 2: Tropical Cyclone Wanda 30
6.2.1 Atmospheric Model Results 30
6.2.2 Ocean Response 33
7. Discussion and Conclusions **36**
References **38**
Acknowledgements **39**
Appendix 1: The Wave Breaking Algorithm **40**
Appendix 2: The Parametric Cyclone Model **42**
Appendix 3: Generalised Pareto Distribution **43**

Executive Summary

The study documented in this report is concerned with evaluating the likelihood of storm tide levels (excluding rainfall runoff and Greenhouse effects) within the Broadwater of the Gold Coast. The two most common and significant classes of severe weather events responsible for storm tides in this region are tropical cyclones and mid-latitude depressions such as east coast lows. This report documents the methodology for determining storm tide levels, which combines deterministic modelling of coastal sea levels using the GEMS Coastal Ocean Model (GCOM2D) with statistical models of cyclone occurrence and east coast low occurrence. Results are obtained at the entrances to the Seaway and the Coomera River.

Storm tide levels are defined as the elevation of water from mean sea level resulting from the effects of tides, winds and waves, excluding any contributions from freshwater runoff, Greenhouse warming of the oceans or changes in future storm climatologies. For the three primary locations of the study, the storm tide levels are as follows:

Summary of predicted storm tide frequencies at three locations.

Location	Return period (years)	Storm tide (m)
Seaway Entrance	50	1.9 ± 0.1
	100	2.1 ± 0.1
Coomera 1 (southern arm)	50	1.8 ± 0.1
	100	1.95 ± 0.1
Coomera 2 (northern arm)	50	1.8 ± 0.1
	100	1.95 ± 0.1

The key findings of the study are:

(1) Coastal-crossing cyclones are the dominant feature for extreme storm tide events, although east coast lows and offshore tropical cyclones have the capacity to generate highly significant events, particularly through generation of large ocean waves.

(2) The capacity to specify accurately the long term storm tide risk is to some extent restricted by the infrequency of extreme cyclone events in the region.

(3) The results of the current study are generally consistent with the results of the Blain et al. (1985) study on the open coastline. However, storm tide levels for 100 year order events inside the Broadwater were found to be of the order 0.1 to 0.15 m lower than storm tide levels on the open coast near the Seaway entrance. At longer return periods (more than 100 years), predicted storm tide levels in the current study are higher than for Blain et al. (1985); this is most likely attributable to the explicit treatment of wave effects in the current study.

Detailed simulations of two events were also undertaken. The first event was an east coast low that occurred in April 1989. This event verified well against available observations. Analysis of the model simulations revealed that wave setup produced a greater contribution to the elevated water levels than the storm surge.

The second case to be modelled was tropical cyclone Wanda, responsible for the 1974 floods. Since rainfall runoff was a major contributor to the floods, GCOM2D incorporated the runoff from the five major river systems that flow into the Broadwater as an additional boundary condition. In addition, the bathymetry in the vicinity of the Seaway was modified to reflect the shallower 1974 depths. Modelled sea levels were reasonably well captured. Sensitivity experiments showed that storm surge and wave setup were only minor contributors to the elevated sea levels and their contribution was confined to the earlier stage of the event before the runoff reached its peak. The contribution due to runoff-only exhibited a tidal-like oscillation that was 180° out-of-phase with the tide; this was attributed to the greater hydraulic resistance that occurs at high tide. A simulation of this event with present day bathymetry at the Seaway produced sea levels that were 0.3-0.4 m lower than the simulation with 1974 bathymetry. This event serves to highlight the fact that severe runoff can considerably worsen or prolong an extreme sea-level event in the Broadwater and efforts should be made to integrate the effects of runoff in future return period analyses.

Disclaimer

Global Environmental Modelling Systems (GEMS), its staff, and any subcontractors used in this study have applied the best techniques available to GEMS to carry out the work. The reader is however advised to take note of the limitations pointed out in the body of the report. GEMS, its staff, and subcontractors take no responsibility for the effect on the results of these, or any other limitations not noted in the report, or for the interpretation or application of these results by other parties.

GEMS has attempted to carry out a scientific study applying methodologies that are an improvement on previous work in this area. This is not to imply however that methodologies cannot be applied in the future which improve upon this work.

Graeme D. Hubbert
Managing Director
March 31, 2000

1. Introduction

The study documented in this report is concerned with evaluating the likelihood of storm tide levels (excluding rainfall runoff and Greenhouse effects) within the Broadwater of the Gold Coast. The two most common and significant classes of severe weather events responsible for storm tides in southern Queensland are tropical cyclones and mid-latitude depressions such as east coast lows. Both types of event are considered in this study. This report documents the methodology for determining storm tide levels and gives the results obtained at the entrances to the Seaway and the Coomera River. In addition to this, the results from a detailed validation exercise involving two case studies are also presented and discussed.

The Gold Coast Broadwater is a large coastal lagoon situated to the north of the Gold Coast (see Figure 1). It is connected to the Pacific Ocean via the Seaway at the southern end of South Stradbroke Island and via a semi-permanent channel at the northern end. A complex network of channels to the west of North Stradbroke Island also connects the Broadwater to the southern end of Moreton Bay.

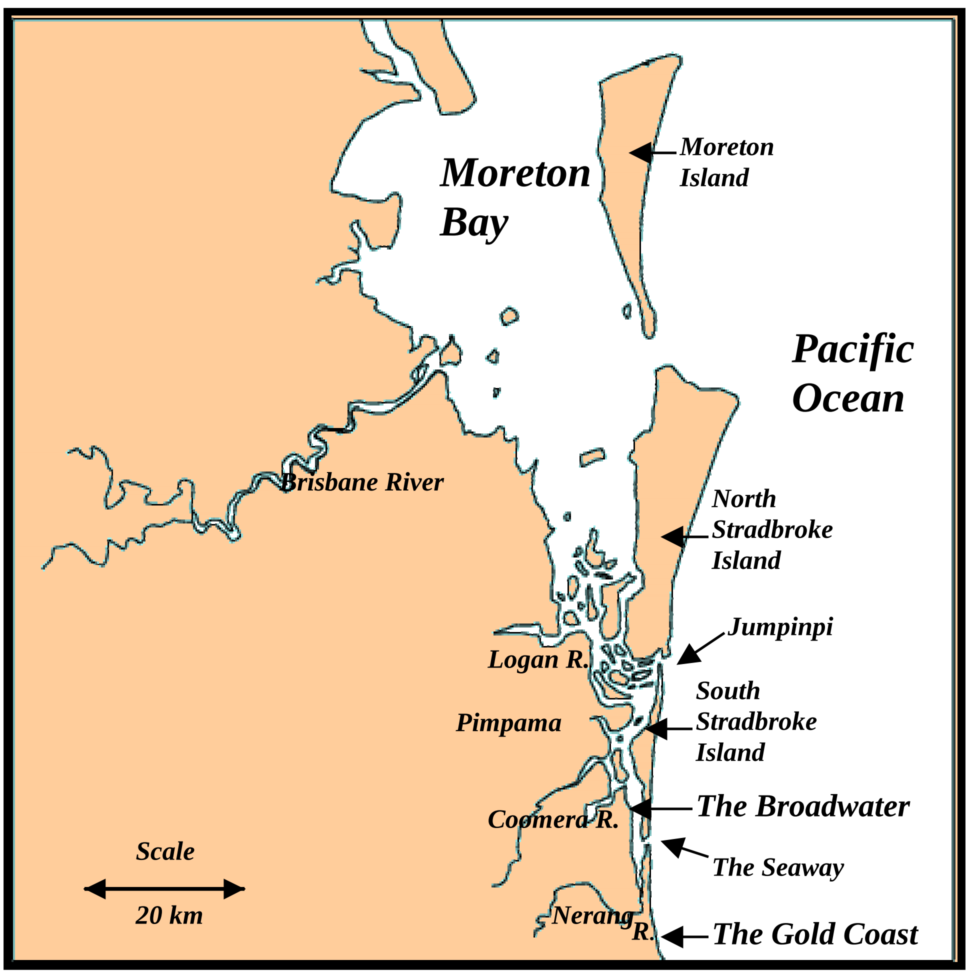

Figure 1: Map of the region.

The Broadwater is an outflow region for a number of major rivers and streams including the Nerang, Coomera, Pimpama and Logan. The floodplains of the Broadwater are extensively developed and a large number of dwellings are at risk of flooding during major flood events. Furthermore, increasing pressure to develop remaining floodplain areas will reduce the floodwater storage capacity during severe flood events. Storm tides within the Broadwater can exacerbate flood events by elevating sea levels at the outflow regions of rivers and streams thereby reducing their flow rates. In many situations, the weather conditions that cause storm tide events are also accompanied by severe rainfall. The establishment of design storm tide levels for planning and development purposes is therefore of critical importance to minimize the risk of damage to infrastructure during such events.

Previous studies conducted in this region have modelled the storm surges resulting from tropical cyclones (Harper et al., 1977), and determined return periods for storm tides (Blain et al., 1985), on the open coastline of the Gold Coast. Hydrological modelling of the Coomera and Nerang river systems that drain into the Broadwater has also been undertaken to establish return periods for peak flow events. No studies to date have attempted to model the complex flows within the Broadwater itself. Design storm tide levels within the Broadwater, up to now, have been derived from those calculated on the open coast by Blain et al. (1985) with an additional contribution due to wave setup added to these levels.

In the present study, the dynamical storm surge model, GCOM2D (Hubbert and McInnes, 1999a, b) has been set up over the entire Broadwater region to model explicitly storm surges and tides in the region. GCOM2D has also been linked to a third generation wave model (The WAMDI Group, 1988). Significant wave heights are therefore explicitly modelled, and enable the wave setup at the coast to be evaluated within GCOM2D and incorporated into the storm tide simulations.

The remainder of this report is set out as follows: in section 2, a discussion of the weather events that affect the region is described. Section 3 describes the various models used in the study. The methodology for evaluating storm tide return periods is described in section 4 and results of the return period analysis are given in section 5. Case studies are presented in section 6 and conclusions are presented in section 7.

2. Extreme Events and Coastal Impacts

2.1 Coastal Effects

Increases in coastal sea levels during severe storm conditions are due to storm surges and breaking waves superimposed on the astronomical tides, as illustrated in Figure 2. Storm surges are generated by wind stresses and, to a lesser extent, falling atmospheric pressure that produces a rise in water level at the rate of approximately 1 cm per hPa fall in pressure (the so-called *inverse barometer effect*). Wind stresses induce ocean currents that, if blocked by a coastal barrier, pile water against the coast to produce elevated sea levels. This process is commonly referred to as *wind setup*. Alternatively, wind stresses acting in the longshore direction with sufficient fetch and duration produce longshore currents that eventually become deflected to the left of the current direction in the Southern Hemisphere due to Coriolis effects. If a coastal barrier blocks the path of the deflected flow, elevated sea levels can also occur due to a process referred to as *current setup* or *Ekman drift*.

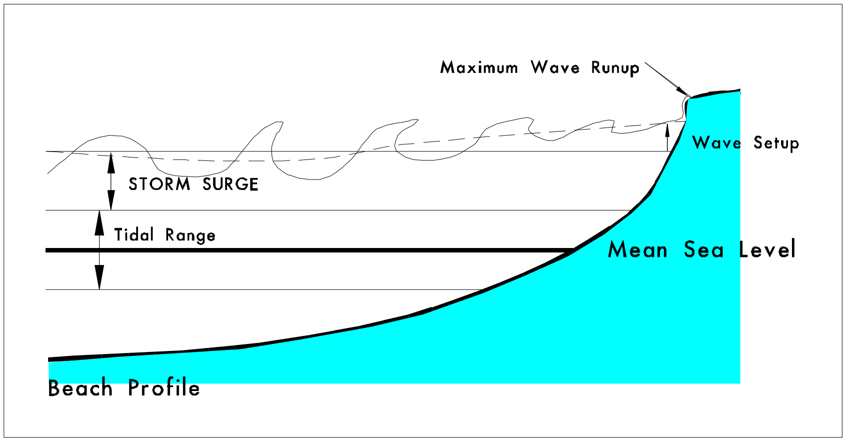

Figure 2: Contributions to extreme sea levels at the coast.

Coastal bathymetry can also affect storm surge intensity. Shallow coastal bathymetry tends to amplify the storm surge while topographic features can channel the coastal currents. Along the southern Queensland coast, the narrow continental shelf is not conducive to large storm surge generation.

Breaking surface waves in the coastal zone cause a change in momentum flux that is balanced by an increase in the still water level and is referred to as wave setup. Wave setup at the coast is a function of wave height and direction at breaking, which is dependent upon the wind direction, strength, duration and fetch as well as the bathymetry in shallow water. The contribution to extreme sea levels along the southern Queensland coast due to wave setup is generally likely to be comparable to the storm surge effect in many circumstances.

Astronomical tides, storm surges and wave setup interact non-linearly to produce total sea levels that are lower than the sum of the individual contributions. This is due to the friction of the ocean floor that has a retarding effect on the flow, and which is proportional to the square of the coastal current. For this reason, it is preferable to integrate the effects of all contributions to coastal currents and sea levels in a dynamical model simulation rather than adding the effects of some components separately at a later stage.

2.2 Meteorology

Southeastern Queensland experiences severe storms from both tropical and sub-tropical regions. Tropical cyclones are potentially the most severe class of storm to affect the region although they are relatively infrequent. Depressions of sub-tropical origin, such as east coast lows, are more frequent but generally less intense than tropical cyclones. However, their larger spatial scale and longer duration suggest that they are likely to be the most frequent contributor to elevated sea-level events in the region. Both storm systems are capable of generating severe rainfall, which if coincident with elevated coastal sea levels, can further increase the likelihood of coastal flooding.

3. Models

The suite of models used in this study includes atmospheric models for generating the meteorological conditions accompanying the storm events, a tidal model, a wave model and the Global Environmental Modelling Systems Pty Ltd (GEMS) storm surge and inundation model GCOM2D. The interaction of the various components is illustrated in Figure 3. The atmospheric conditions for coast-crossing and coast-parallel cyclones are derived from a cyclone vortex model whereas those used for off-shore cyclones and east coast lows are obtained from the U.S. National Center for Environmental Prediction (NCEP) global analyses. For the detailed case studies, the Colorado State University non-hydrostatic Regional Atmospheric Modelling System (RAMS) was used. Tidal forcing is required only for the coarse resolution ocean model simulation. The output of this simulation therefore contains sea levels and currents that are due to both meteorological and tidal components and supplies the boundary conditions for the higher resolution ocean model simulation (see Figure 4).

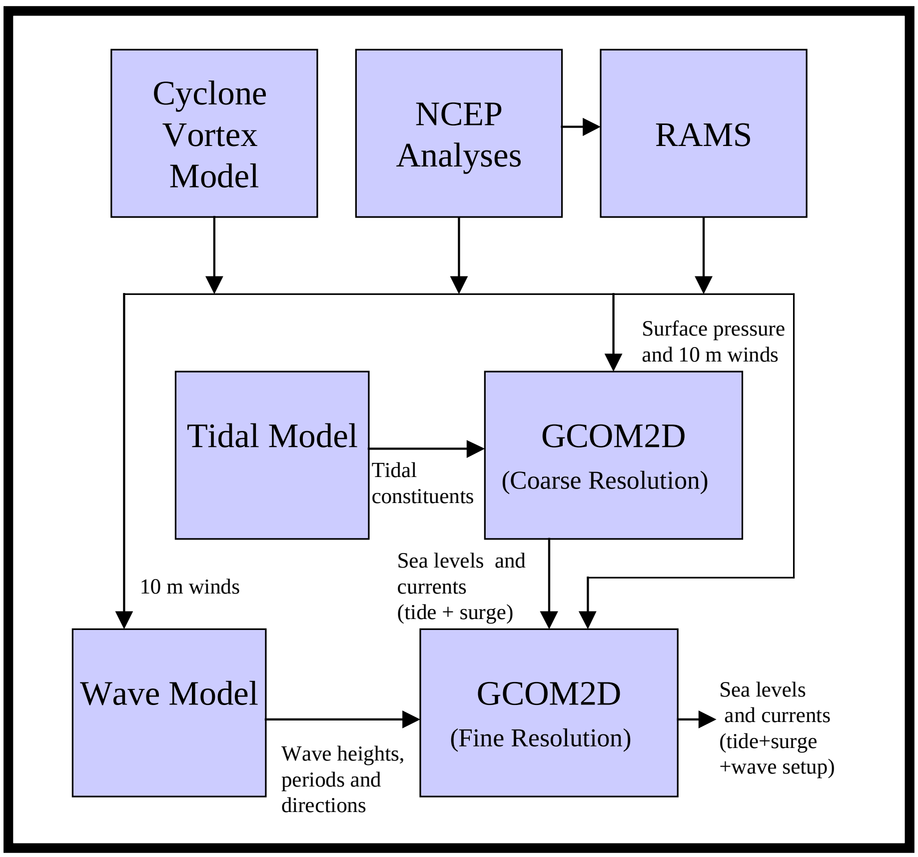

Figure 3: Diagram illustrating the modelling system used in the study.

3.1 Storm Surge Model

The coastal ocean model, GCOM2D (Hubbert and McInnes, 1999a,b) solves the depth-averaged hydrodynamic equations over a region defined by detailed topographic and bathymetric information to provide currents, sea-level heights and overland flow of water due to tidal and meteorological conditions. The inundation algorithm floods and dries at rates that are dependent on the modelled currents. It has been shown that sea levels simulated at the coast are more realistic when a moveable coastal boundary is used, compared to the simpler to implement, fixed-coast storm surge models that tend to overestimate the coastal sea levels (Yeh and Chou, 1979; Hubbert and McInnes, 1999a,b).

GCOM2D features a grid generator to facilitate the setting up of model grids over any specified geographical region and grid resolution. It can be run over successively higher resolution regions utilising the results of lower resolution, outer simulations as boundary conditions. This so-called 'nesting' technique is an economical way of maximizing grid resolution while maintaining reasonable computational overheads. The user interface is capable of incorporating output from a wide range of atmospheric models to obtain surface winds and pressure.

In the present study, GCOM2D is run over the two regions illustrated in Figure 4. The larger lower resolution region has a horizontal grid spacing of 1.0 km, while the smaller inner region has a grid resolution of 100 m. Atmospheric and tidal forcing is applied to the coarse resolution simulations. The sea-level elevations from the coarse resolution simulations are applied at the lateral boundaries of the fine resolution simulations. Atmospheric forcing is also applied to the fine resolution simulations.

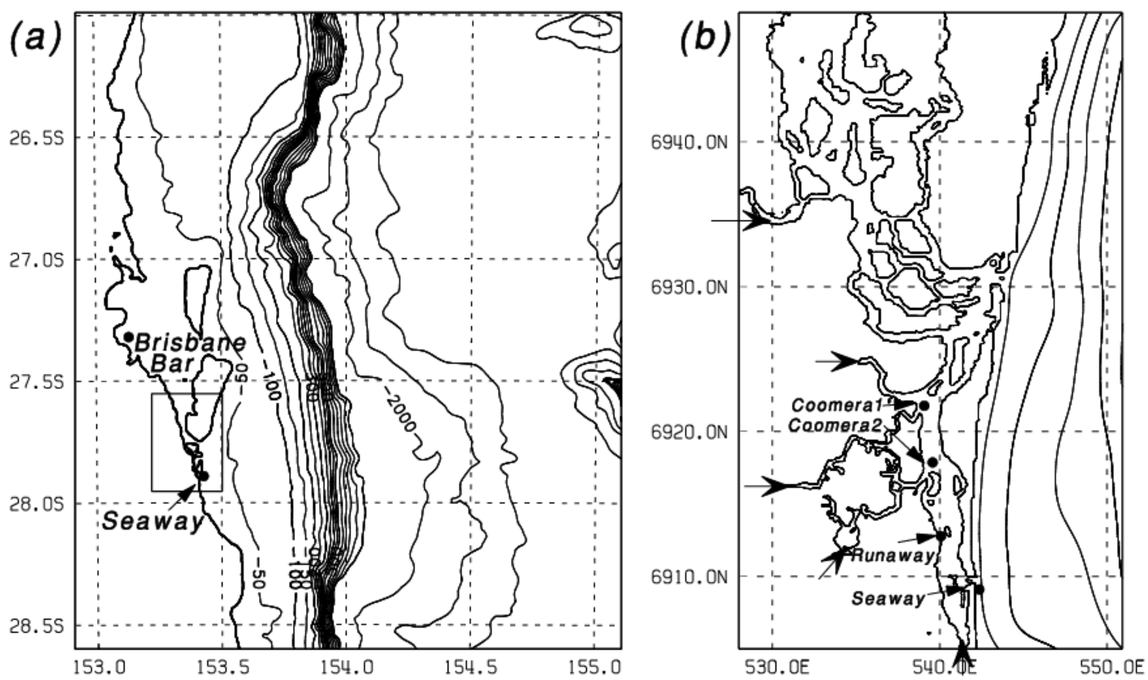

Figure 4: (a) Coarse 1500-m resolution (140×188 gridpoints) and (b) fine 100-m resolution (230×440 gridpoints) topographical grid used by GCOM2D. Bathymetric contours on (a) are shown every 50 m up to 500 m and then 500-m intervals thereafter and on (b) every 5 m. Locations used throughout the report are marked, as are the river inflow points for the 1974 flood event. (Note: The wave model was run on a larger open ocean grid).

Meteorological conditions required by GCOM2D consist of the 10-m winds and surface pressure and are derived from either a cyclone model, archived analyses or regional atmospheric model simulations (see section 3.2). They are interpolated both spatially and temporally from the atmospheric model grid to the GCOM2D coarse and fine mesh grids.

The tidal prediction model reads the astronomical constants for each tidal constituent and calculates the tidal heights. These are applied as lateral boundary conditions in the coarse resolution GCOM2D simulation.

The effect of ocean waves is incorpored via a wave radiation stress term (see section 3.2 and Appendix 1) in the momentum equations. The radiation stresses are calculated from the wave heights in the surf zone.

3.2 Wave Model

It is now well known that the action of breaking waves produces a shoreward momentum flux, which leads to a mean increase in water level (known as wave setup) in the breaking wave zone. Battjes and Janssen (1978) developed a one-dimensional model to simulate this process by combining a bore-type dissipation model with a probabilistic model to allow for random variation in wave heights. The model allows calculation of wave setup shoreward based on the wave height outside the breaking zone and the variation of bathymetry. The calculated wave setup can then be added to the modelled water levels due to tides and surge. This model approach has been used in a study of the relative contributions to east coast sea-level anomalies cause by east cost lows (McInnes and Hubbert, 2000).

In terms of two-dimensional coastal ocean modelling, a more general approach is to include the effects of wave setup via the horizontal gradients of the wave radiation stress terms in the hydrodynamic model. These can be incorporated as an extra forcing term analogous to the wind stress term in the horizontal momentum equations (see, for example, Mastenbroek et al., 1993). The wave setup algorithm used in GCOM2D is described in Appendix 1.

The wave parameters (height, direction and period) required for the radiation stress calculation are simulated using the third generation spectral ocean wave model (The WAMDI Group, 1988). The wave model is run over a region spanning 26° S to 29.25° S and 152.8° E to 156° E at a resolution of 0.05° (approximately 5 km). Time series of the wave parameters (height, period, direction) are then interpolated to the GCOM2D fine grid.

The approach adopted allows treatment of the wave stresses in two dimensions which is found to be important in accurately representing sea level heights due to wave setup. In cyclone cases, where the most extreme winds are at an angle to the coast, a significant proportion of the wave energy may propagate ‘along shore’ and provide little or no contribution to sea-level increase. Earlier studies employing a ‘one-dimensional’ approach, based on the wave height alone, will tend to have overestimated the contribution of wave setup in such cases.

3.3 Atmospheric Fields

For the purposes of this study, meteorological forcing for extreme storm tide events in the return period analysis is divided into two categories. The first is near-shore tropical cyclones (both coast-crossing and coast-parallel) and the second is offshore cyclones and east coast lows. The meteorological forcing for each class of event is derived from a different source as outlined below.

3.3.1 Cyclone Model

Surface pressure and 10-m wind fields for coast-crossing and coast-parallel tropical cyclone events are generated using an analytical wind field model based on Holland (1980) as described in Hubbert et al. (1991) (see Appendix 2 for details).

It is important to note that the tropical cyclone model is not expected to represent the full field of synoptic scale features with a high degree of accuracy. The critical aspect for storm surge and wave forcing is that the model parameterises the mesoscale forcing in the vicinity of the maximum winds reasonably well.

3.3.2 NCEP Analyses

Offshore tropical cyclones and east-coast low events are not likely to produce a significant storm surge but due to their often long duration and large spatial scale, these events can generate large waves offshore leading to wave setup at the coast. Atmospheric fields for this class of events were obtained from an archive of reanalysed data produced by the U.S. National Center for Environmental Prediction (NCEP) available on a 1.875º $\times$ 1.875º global grid for 10-m winds and on a 2.5º $\times$ 2.5º global grid for mean sea level pressure. The global data are available every 6 hours from 1958 to 1997.

3.3.3 Regional Atmospheric Modelling System (RAMS)

In the verification studies presented in section 6, a high resolution atmospheric model is used to generate the wind and pressure fields The atmospheric numerical model used in this study is the Colorado State University Regional Atmospheric Modelling System (RAMS). Details of the RAMS model can be found in Tremback et al. (1986).

RAMS is a 3-dimensional, non-hydrostatic, nested numerical model able to represent the updraft/downdraft cores usually associated with extreme precipitation events. The characteristics of these cores require that the model must explicitly model the vertical accelerations in the atmosphere. This type of model is referred to as “non-hydrostatic” since it does not invoke the hydrostatic approximation concerning vertical motion (i.e. the hydrostatic assumption neglects vertical motions). The updraft/downdraft cores are embedded in larger synoptic systems that also must be represented by the model. The computing requirements to model the full extent of the synoptic system at a horizontal resolution of 1-2 km is prohibitive. The model must therefore be nested; that is, the large-scale flow must be modelled at lower resolution and used to force the boundaries of the high resolution simulation.

Physical processes represented by the model include important surface processes such as evaporation and surface heating. The effects of radiation therefore include the diurnal heating and cooling cycle, as well as the interaction of the longwave and shortwave radiation with the clouds. Mixing in the boundary layer takes account of turbulent mixing and shallow convection. Deep convection and cloud- and rain-generating processes in the atmosphere are also considered.

In the simulations discussed here, the numerical model has been initialized using NCEP analyses. These analyses are interpolated horizontally and vertically to the outer model grid that has a resolution of 45 km. The analyses also provide the temporal forcing on the lateral boundaries of the outer model grid. Three levels of interactive grid nesting were used, the middle and finest resolution grids having a horizontal grid spacing of 15 km and 5 km respectively. The terrain used on all model grids was interpolated from a 1/40th degree data set. The sea surface temperatures (SST) were obtained from the NCEP analyses.

4. Methodology for Evaluating Storm tide Statistics

In this study, storm tides resulting from near-shore tropical cyclones have been treated separately from those resulting from east coast lows or tropical cyclones that are located well offshore. For the nearshore tropical cyclones, a synthetic storm tide record is generated using a Monte-Carlo method, which entails performing many storm tide simulations from randomly selected cyclone characteristics. The simulated storm tides are then analysed directly to produce return periods.

For east coast lows and offshore tropical cyclones, 34 actual events are simulated. This approach was preferred to the Monte-Carlo method for the east coast lows and offshore cyclones because of the difficulty in representing storms tracks and the absence of representative models for defining the wind fields associated with the events.

4.1 Near-shore and Coast-Crossing Tropical Cyclones

The magnitude of the storm surge resulting from a tropical cyclone depends on the following factors:

- *intensity* of the cyclone's central pressure
- *size* (measured by the radius from the cyclone centre to the region of maximum winds)
- *track* including its direction of movement, forward speed and proximity to the point of interest
- *depth* and *shape* of the ocean floor.

The methodology for generating storm tide return periods requires simulating a large number of storm tides from cyclones that are randomly selected from weighted frequency distributions of cyclone characteristics. The frequency distributions are determined by fitting distribution functions to the distributions of *observed* cyclone characteristics in the Gold Coast region.

4.1.1 Cyclone Intensity

Prediction of long-term storm intensity for the southeast Queensland region is problematic because of the relative infrequency of severe tropical storms. Cyclone intensity is principally related to storm central pressure although the strength of the winds is also related to the forward speed of the system. In this study, storm intensity was based on the central pressure of cyclones occurring in the region bounded by 26 to 30º S and 152 to 155º E. Although the cyclone data base dates to 1908, cyclones occurring in the pre-satellite era (prior to about 1960) are generally considered to be less quantitatively reliable. However, in the interests of obtaining a sufficient number of events to perform a meaningful statistical analysis in the present study, cyclones were selected from the 1953 to 1997 seasons inclusive. These cyclones are referred to as 'southeast Queensland storms'.

The lowest central pressure in the region occurred with 'Dinah' in 1967 at about 950 hPa (Dinah's central pressure was estimated at 945 hPa just north of the region). Although this particular storm had re-curved by the time it entered the study region, Bureau of Meteorology advice suggests that a favorable synoptic situation would allow such a storm to track on to the southeast Queensland coast, maintaining its intensity (J. Callaghan, private communication, 1998). Figure 5 shows the location of the selected storms at the time of their maximum intensity.

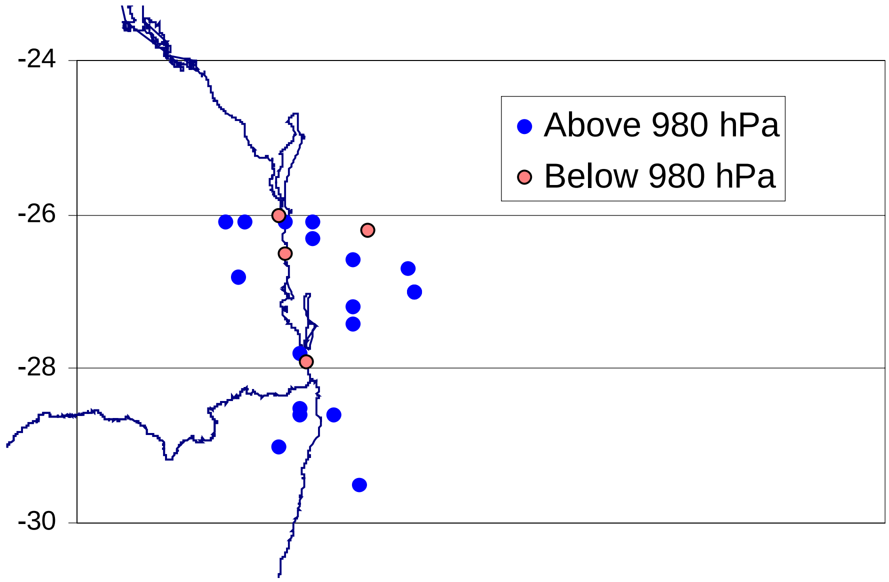

Figure 5: Location of 'southeast Queensland storms' at the time of maximum intensity.

Figure 6 shows a frequency distribution of storm intensity (as measured by cyclone central pressure). The storm central pressures were subject to analysis with the Generalized Pareto Method (see Appendix 3) to determine appropriate recurrence probabilities. Figure 7 shows these recurrence probabilities expressed as return periods for the southeast Queensland storms.

Figure 6: Frequency distribution of storm pressures

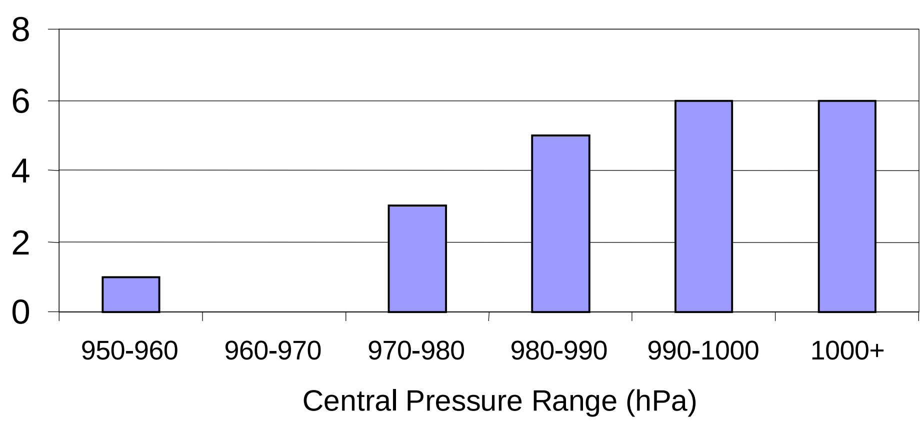

Return periods for storms affecting the Gold Coast (defined as storms within a region from which measurable storm surge could be expected) were based on the southeast Queensland storms pressure distribution modified for the mean number of cyclones within the Gold Coast storm surge region (26° S to 28.0° S). This modified distribution (again expressed as return periods) is also shown in Figure 7.

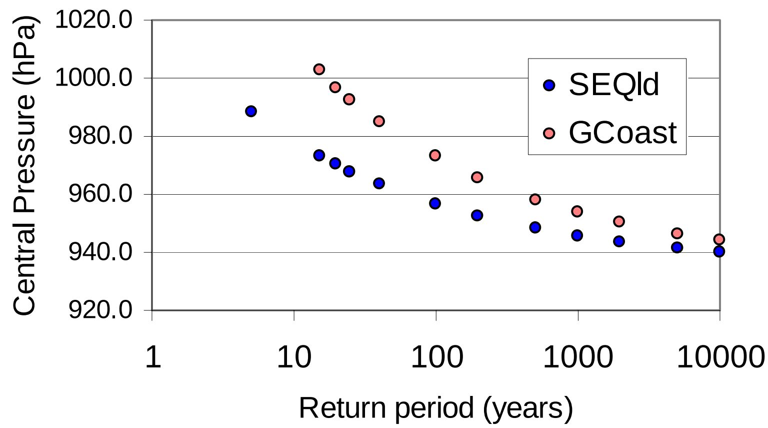

Figure 7: Probability distributions of tropical cyclone pressure for storms in the southeast Queensland region (bounded by 26 to 30°S and 152 to 155°E) and the Gold Coast region (bounded by 26 to 28°S and 153 to 155°E) expressed as return periods.

4.1.2 Cyclone Tracks

The distribution functions for cyclone direction and speed for the coastal crossing and near coast storms were fitted to the actual frequency distributions of cyclone direction and speed. The direction and speed values that were used were the average of the observed values over the 12 hours leading up to the cyclone crossing the coast.

Figure 8 shows the fitted distribution for storm direction where the cyclone is moving ‘from’ the given direction. Storms in the range 345°-360° represent those storms that move approximately parallel to the coast. Figure 9 shows the fitted distribution of storm speed. Cyclone crossing locations were assumed to vary from 25.5°S to 28°S with equal likelihood of occurrence.

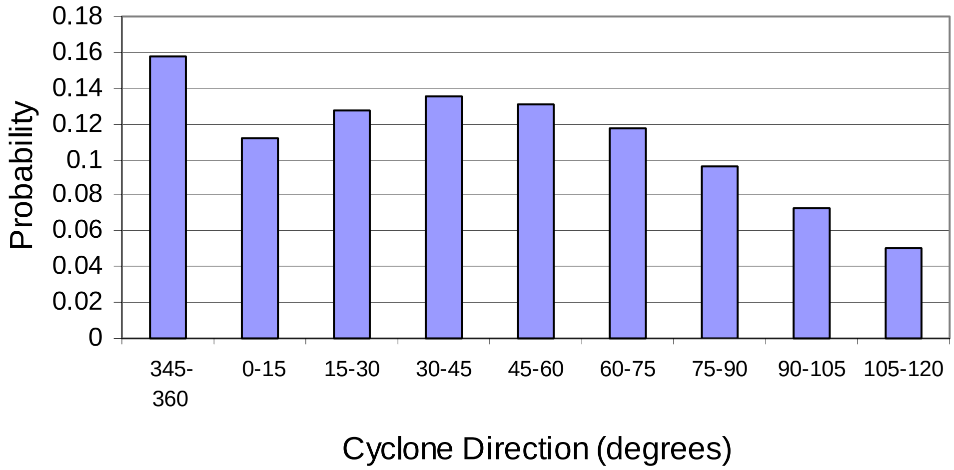

Figure 8: Distribution of storm directions, Gold Coast region.

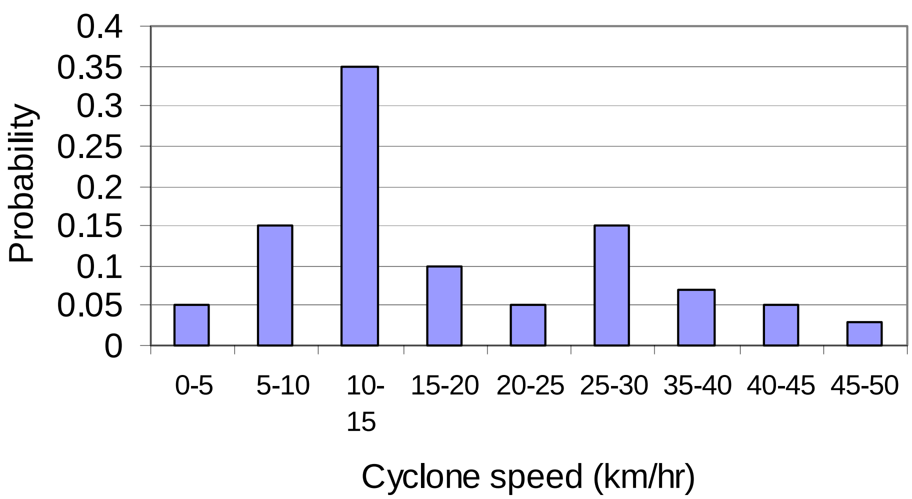

Figure 9: Distribution of storm speed, Gold Coast region.

4.1.3 Modelling the Storm tides

Individual cyclone characteristics, including storm track and intensity, were randomly selected and used to generate synthetic cyclones that were then used to drive the storm surge model. The range of possible cyclone characteristics were limited by the bounds of the probability density functions presented in the previous two sections.

This process involves:

- randomly selecting a start date during the cyclone season, which is then used to initialise the tidal model
- randomly selecting a storm central pressure and speed of movement
- randomly selecting a ‘coastal crossing location’
- running the cyclone model
- running the storm surge model.

By making a large number of such simulations the climatology of the synthetic cyclones matches that of the observed cyclones but the number of events is increased. The synthetic data set of predicted sea-level peaks then provides a much more complete representation of possible storm tide combinations. The synthetic data are then subject to analysis (see next section) to determine appropriate return periods of sea level.

4.2 Offshore Tropical Cyclones and East Coast Lows

4.2.1 Selection of Atmospheric Conditions

The cyclone vortex model cannot adequately represent the broadscale wind field outside the region of most intense winds, and this is particularly the case where a cyclone interacts with the sub-tropical ridge to produce an extensive region of strong onshore winds. Where the wind remains strong for a period of the order of days, large swells can develop with the potential to produce significant sea-level elevations through the process of wave setup. This process is compounded when the cyclone centre approaches the coast causing a more localised increase in wave setup and some storm surge.

There can be a similar interaction between developing east coast lows and an underlying ridge to produce broad onshore flow as well as a localised wind maximum on the southern or southeastern flank of the low centre. This process is also not well represented by a cyclone vortex model.

To better represent the winds in such cases, winds from the NCEP analyses were used to drive the ocean models for these types of events. The relatively large grid spacing of the stored wind data means that the finer detail of some of these systems is not well represented. Ideally, the NCEP atmospheric fields would be used to initialize a high resolution, limited area atmospheric model; however, the time constraints of the current project did not allow such an approach to be used. Instead the NCEP winds were modified through manual analysis on the basis of available coastal and ship based observations.

Events for study were selected from the 20-year period from 1977 to 1996 inclusive. This period was chosen as it coincides with a period for which wave height data are available for a site off North Stradbroke Island. A study of the wave records from this site (Allan and Callaghan, 2000) identified the governing synoptic conditions for each significant event, with the more extreme events associated with east coast lows and to a lesser extent tropical cyclones. A selection of the most severe events on the basis of recorded wave heights was made on the assumption that this would identify the most significant storm events affecting the region and it was found from modelling these events that this indeed was the case. It was also found that the inclusion of wave direction was important for correctly simulating the contribution to the total sea levels due to wave setup.

4.2.2 Modelling the Storm tides

The modelling sequence for the offshore tropical cyclones and east coast lows paralleled that for the coastal tropical cyclones except that the governing wind fields were derived from the modified NCEP analyses.

The modelled events were run with tidal forcing and the residual sea levels due to the storm surge and wave setup then extracted for analysis. For several events occurring from 1989 onwards, model predictions were verified against data available from the Queensland Department of Transport tide gauge at the Gold Coast Seaway. For these cases output for the model seaway tag point, which was slightly offshore from the Seaway, were on average slightly higher (order 0.1 m) compared with the tide gauge. Levels at Coomera 2 in these events were similarly lower than the open coast tag point so that the predicted Coomera 2 and tide gauge readings were generally similar. This is reasonable, since the tide gauge is inside the entrance to the Seaway and tidal attenuation would largely have taken place by this time.

Investigations undertaken for this report confirm that for most of these events, wave action causes the major contribution to sea-level increase. The importance of wave direction is demonstrated by the significant variation in sea-level elevation residuals for events with similar maximum wave heights but different directions.

4.3 Event Probability: Return Periods of Sea Level

In previous sections of this report the processes that contribute to sea-level increase at the Gold Coast and the methodologies for modelling these processes were considered. In this section we describe how probabilities for the occurrence of these events have been determined.

By convention, the *return period* of an event is the period of time over which the event might be expected, on average, to occur once. Here ‘an event’ is defined as the sea level *exceeding* a particular height.

Mathematically, the return period is determined as the inverse of the probability of a particular event occurring,

$$R_L = 1/\Pr \text{(sea level exceeding level L in any year).} \qquad (1)$$

The return period does *not* represent an estimate of the period until the *next* event. It is possible, for example, that two “100 year” events might occur one year after another. However, over a longer period of time, i.e. many thousands of years, it would be expected that this event would occur on average once every 100 years.

Predictions for the return period based on the tropical cyclone storm tide events were made by applying the Generalized Pareto Method to the simulated sea levels at the three tag points (as described in Appendix 3).

Due to the relatively small number of actual east coast low and offshore tropical cyclone events simulated, a different approach was used to evaluate the return periods of these events. Firstly the tidal component of the sea level was removed from the simulations. The reason it was included in the first place is that the total sea level obtained by integrating storm surge, wave setup and tidal effects together is lower than the sum of the individual components had they been modelled separately and then summed together. This is due to the non-linear retarding effect of the friction of the ocean floor on the water currents. Therefore a more realistic simulation of the storm surge and wave setup components (the residual sea level) is obtained by including tides and then subtracting them out later (as indeed is the case when sea-level residuals are obtained from tide gauge records).

The residual sea-level data were then subjected to extreme value analysis to obtain the frequency distribution of the storm component of sea level for these events. These data were then combined with tidal forcing through a joint probability analysis and annual return periods calculated accordingly. Sea levels for the offshore cyclones and east coast lows were found to be lower for given return periods compared to tropical cyclones, although they have the capacity to produce extreme events.

5. Results

5.1 Coastal-Crossing Cyclones

A total of 592 cyclone simulations were made. Based on the mean number of cyclone crossings expected per year along the coastline bounded by 25.5º S and 28º S, this corresponds to a period of approximately 3000 years.

Peak storm tide estimates at the three locations were obtained from each simulation. These simulations represent a wide range of tropical cyclone events interacting with randomly generated tidal phases. Figure 10 shows the return period estimates derived for the Seaway and Coomera-1. The results for Coomera-2 are similar to those for Coomera-1 and are therefore not shown.

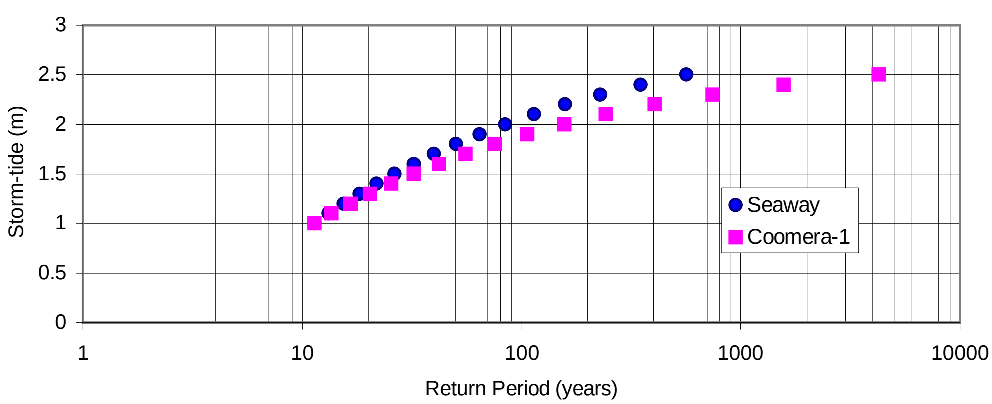

Figure 10. Return period of sea level at the Seaway and Coomera-1 for coastal tropical cyclones.

The results indicate that water levels are slightly higher at the Seaway compared with locations inside the Broadwater. The 100-year prediction for the Seaway is 2.05 m compared with about 1.9 m for Coomera 1 and 2. The Generalized Pareto Method suggests an upper limit of about 3.0 m for the Seaway, which corresponds to a storm around 940 hPa crossing directly over the region at Highest Astronomical Tide.

5.2 Offshore Tropical Cyclones and East Coast Lows

The residual storm surge (that is the increase in sea level above normal tide) for each of the actual offshore and east coast low events were also subjected to analysis using the Generalized Pareto Method. Figure 11 shows the predictions of the residual versus return period for these types of events at the Seaway. Similar analyses were carried out for Coomera 1 and 2 but the difference between the three locations is small.

The effect of combining tide with these events was achieved by undertaking a joint probability analysis using the results shown in Figure 11 and an analysis of tide exceedance (see Figure 12).

The combined offshore/east coast low storm tide return periods for the Seaway are shown in Figure 13. Comparing these results with those for the coastal crossing cyclones (Figure 10) is instructive. At lower return periods the wave-dominated east coast lows and offshore cyclones produce relatively higher sea levels. However, as return period increases, the less common but more extreme tropical cyclone events tend to dominate.

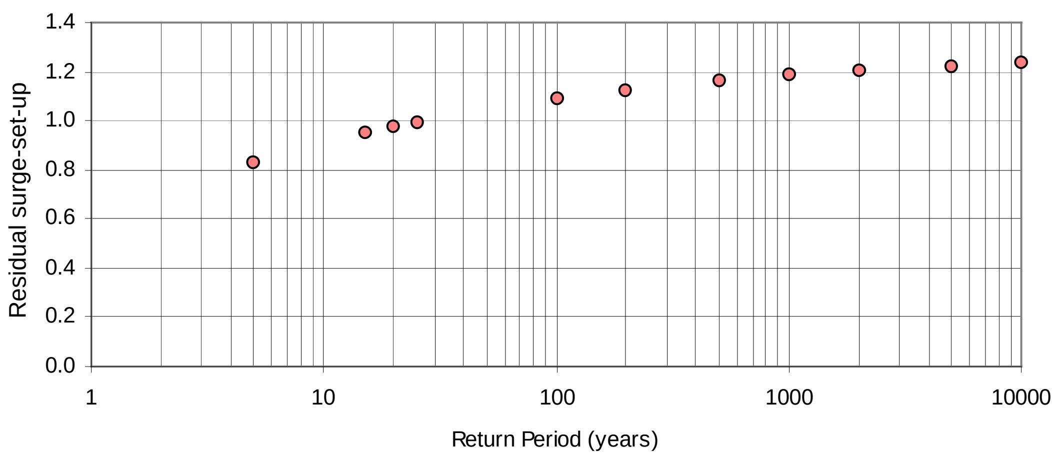

Figure 11. Predicted return period of residual water level (surge + wave setup) for east coast low and ‘offshore’ tropical cyclone events.

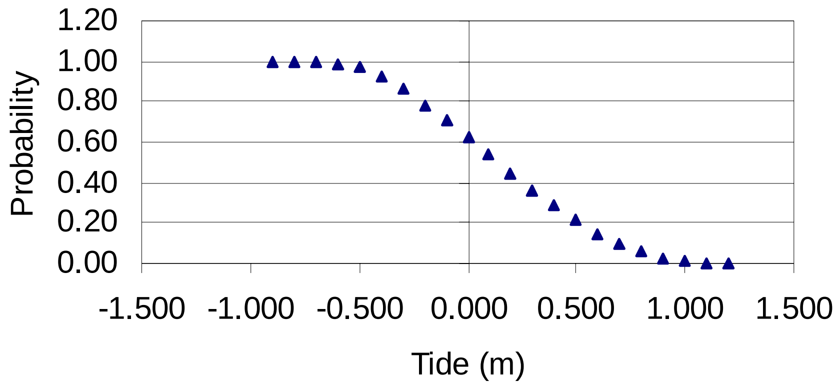

Figure 12. Exceedance probability distribution for Gold Coast tides.

In Figure 13 it can be seen that there appears to be an upper limit of approximately 2.4 m for these events. Given that wave setup appears to provide the dominant forcing in such events such a value seems reasonable. For a highest astronomical tide of 1.2 m, the combined surge and setup would also need to be of the order 1.2 m. Given that the surge contribution in such events is quite low (order 0.1 to 0.2 m) a setup contribution of 1.0 m is implied. Depending on the empirical values used to determine setup from significant wave height, a maximum wave height of about 10 m is implied.

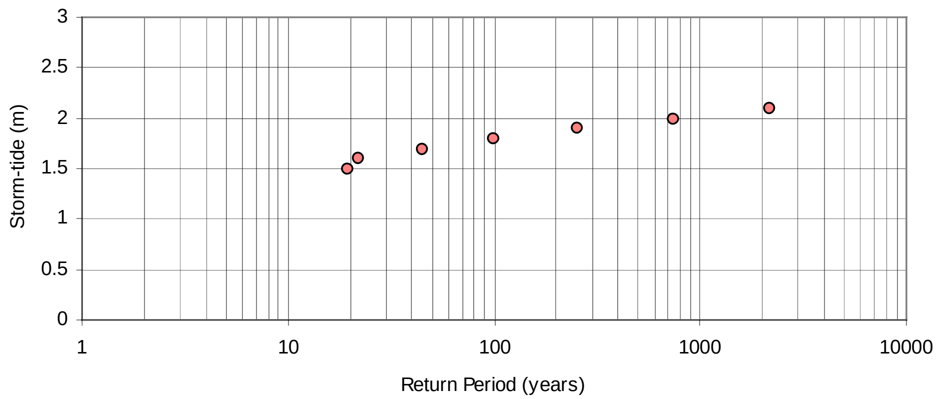

Figure 13. Predicted return period of storm tide combination at the Gold Coast Seaway resulting from effects of east coast lows and distant tropical cyclones.

5.3 Combined Sea-Level Predictions

A combined distribution for storm tide at three locations (entrance to the Seaway, Coomera 1 and Coomera 2), was calculated by calculating the sum of the mean crossing rates of the level of interest, S_R,

$$\lambda_{cc}[1 - F_{cc}(S_R)] + \lambda_{oe}[1 - F_{oe}(S_R)] \qquad (2)$$

where λ_{cc} and λ_{oe} are respectively the mean event frequency of the coastal crossing and offshore and east coast low populations, and F_{cc} and F_{oe} are the non-exceedance probability distributions of the two populations. These parameters are extracted from the analysis described in the previous two sections.

Figure 14 shows the combined distributions for the Gold Coast Seaway and Coomera 1 . The results for Coomera-1 and Coomera-2 are very similar.

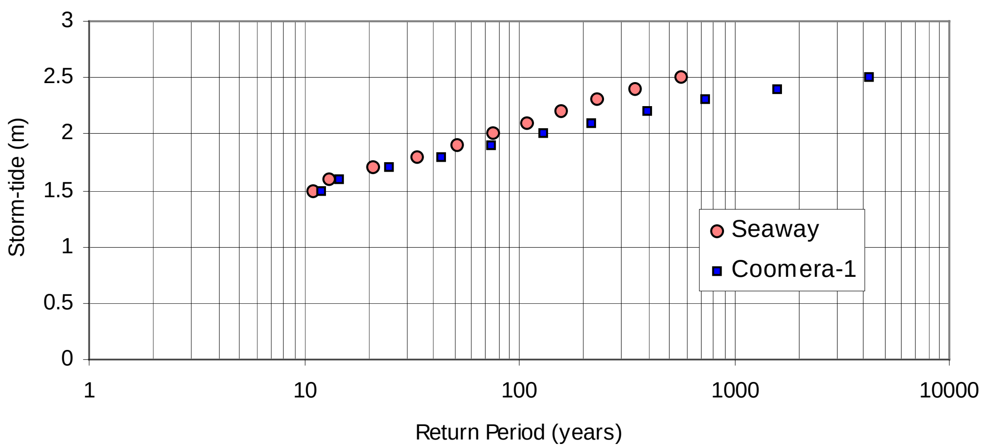

Figure 14. Combined predictions of return periods of sea level for combined effects of coastal tropical cyclones, east coast low and distant cyclones. The 50- and 100-year results derived from this analysis are shown in Table 1.

5.4 Discussion

In the current study we have set out to quantify the sea-level height at specific recurrence intervals with particular emphasis on the 50- and 100-year sea levels. It is important to understand that any given sea-level event may be caused by a range of possible events; for example, a level of, say, 1.6 m may be produced by waves from an east coast low combining with a spring tide or by a significant storm surge combining with a neap tide. The storm surge itself will be dependent on the intensity of the cyclone and how close it passes to the location of interest. There is in fact a spectrum of event combinations that can produce a particular sea level and the aim of the probability analysis is to aggregate the probabilities associated with all possible events. Consequently it is not possible to define a unique event associated with a given return period.

5.5 Uncertainty Estimates

The main contributions to uncertainty in the predicted return periods are:

- The relative infrequency of major cyclone events in the region and associated uncertainty in selection of storm intensity characteristics
- Error in the wind fields used to drive the ocean models
- Lack of directional wave data for calibration of wave effects
- The relatively short duration of reliable records for east coast low events.

Aggregated error estimates were determined by applying mean modelling errors of 0.1m and 0.2 m for the coastal cyclone and east coast low/offshore events respectively. These mean errors were estimated on the basis of verification studies undertaken in the current study and previous studies in other parts of Australia.

Gaussian distributions around the mean errors were numerically applied on a random basis and RMS error calculated for the predicted sea levels.

We note that these error estimates do not include potential error arising from the limitations of the cyclone data base. The predictions are based on best fit to the available data in accordance with normal practice.

The results in Table 1 do not take into account any contributions from freshwater runoff, Greenhouse warming of the oceans or changes in future storm climatologies due to Greenhouse or other effects.

Table 1: Summary of predicted storm tide frequencies at three locations.

Location	Return period (years)	Combined Distribution (m)
Seaway Entrance	50	1.9 ± 0.1
	100	2.1 ± 0.15
Coomera 1 (northern arm)	50	1.8 ± 0.1
	100	1.95 ± 0.15
Coomera 2 (southern arm)	50	1.8 ± 0.1
	100	1.95 ± 0.15

5.6 Comparison with Earlier Studies

The Blain et al. (1985) study quotes 1.3 m and 1.5 m for the 1-in-100 and 1-in -500 year events respectively. The difference between these results and the current study is largely accounted for by the inclusion of wave setup. In this study we have incorporated the setup process directly, by modelling wave heights and calculating wave radiation stresses for direct incorporation into GCOM2D. Since this approach integrates the effects of setup for each event, there is no single estimate of wave setup at a particular recurrence level. Simple addition of a constant value for wave setup must be subject to error. However, in terms of order of magnitude estimates, we note that Callaghan estimates the 100-year significant wave height off Brisbane to be 7.95 m. Given that the 100-year wave is likely to be associated with a significant cyclone or possibly east coast low event, applying a typical estimator of 10 per cent of the offshore wave height gives a reasonable first approximation of 0.8 m for setup. The difference between the results of the earlier study is well within this basic estimate. We note that in a report by Harper (1999), a 100-year setup value of 0.48 m has been applied to the original Blain et al. (1985) storm tide estimate. This value now seems low and may not have allowed for the variability of changing water levels and wave heights that occur during storm tide events.

A small difference (order 0.1m) from the results of Blain et al., (1985) can be attributed to revised predictions of tidal conditions. Other differences may also be expected to result from differences in the storm data bases used for the cyclones and east coast lows (extra-tropical storms) and the treatment of the wind field, particularly for the east coast low events. The Blain et al. (1985) study used a vortex model for such events whereas in the current study more realistic wind fields were applied based on stored numerical model fields.

6. Case Studies

In this section, two severe events are modelled in detail and the results are presented and discussed. The first event is studied to illustrate the running and the performance of the modelling system used in this study. An investigation of the relative sources of storm tide and flood waters in the Broadwater is undertaken and the key sources of error are identified. The second event involves reconstructing the processes contributing to the 1974 floods in the Broadwater. Since the rainfall was a major contributing factor to the floods in this event, GCOM2D was modified to include the flow from the major rivers flowing into the Broadwater. In 1974 the Gold Coast Seaway consisted of a much shallower channel situated to the north of its present day location. The bathymetric data used in GCOM2D were modified to incorporate this difference. This event is also simulated with the present day bathymetry.

6.1 Case 1: 25 April 1989

This event commenced as a tropical low some five hundred km north of the Gold Coast on 24 April. The low subsequently travelled south along the coast finally to be located to the east of the Gold Coast early on 26 April. Gale to storm force winds caused severe erosion along the Sunshine coast while heavy rainfall produced widespread flooding. Sea levels peaked at 0.43 m and 0.5 m above predicted tidal levels in the Broadwater and at Brisbane Bar respectively.

6.1.1 Atmospheric Model Results

A three-day simulation of this event commencing at 0000 UTC 23 April 1989 was performed using the RAMS atmospheric model. Figure 15 shows the Mean Sea Level Pressure (MSLP) during the final 24 hours of the simulation along with verifying analyses from the Bureau of Meteorology. At 0000 UTC 25 April (Figure 15a) the simulated low is deeper and situated slightly further to the south than indicated in the analyses although the pressure gradient along the Gold Coast is generally well captured. At 1200 UTC there is closer agreement in the location and intensity of the low in the vicinity of the Gold Coast.

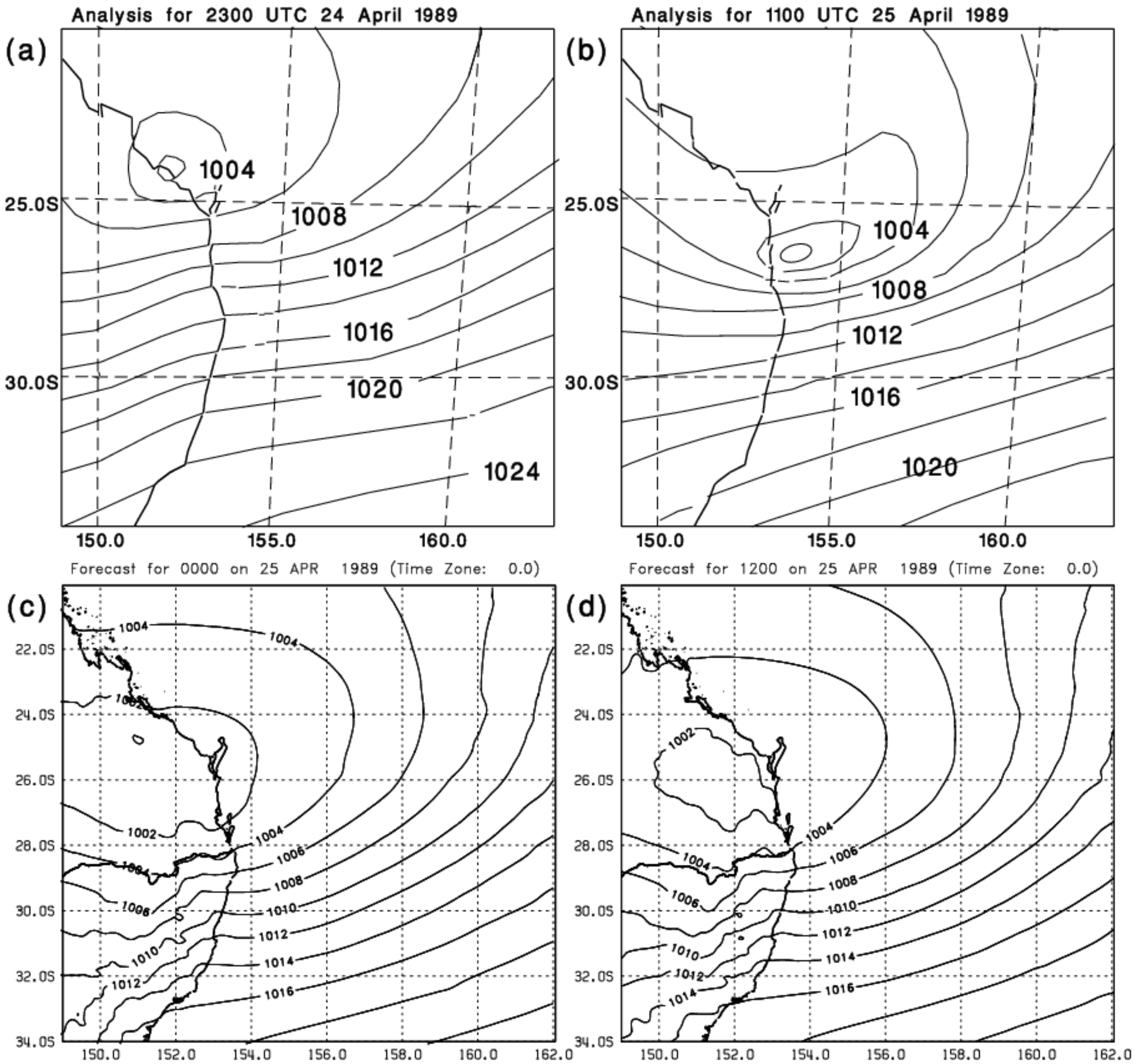

Figure 15: (a) and (b) Manually drawn Bureau of Meteorology analyses at 0000 UTC and 1200 UTC 25 April 1989 respectively, and (c) and (d) RAMS model simulation conducted at 15-km resolution at the corresponding times.

Modelled wind speed and direction are compared with three hourly observations at Cape Moreton and the Gold Coast in Figure 16. Modelled winds at Cape Moreton are weaker than observations particularly in the latter 24 hours of the simulation. This is consistent with the modelled depression being located further to the south at around this time. Closer agreement can be seen at the Gold Coast. Wind direction indicates sustained easterly flow for the first 60 hours at both locations and this is well captured by the model.

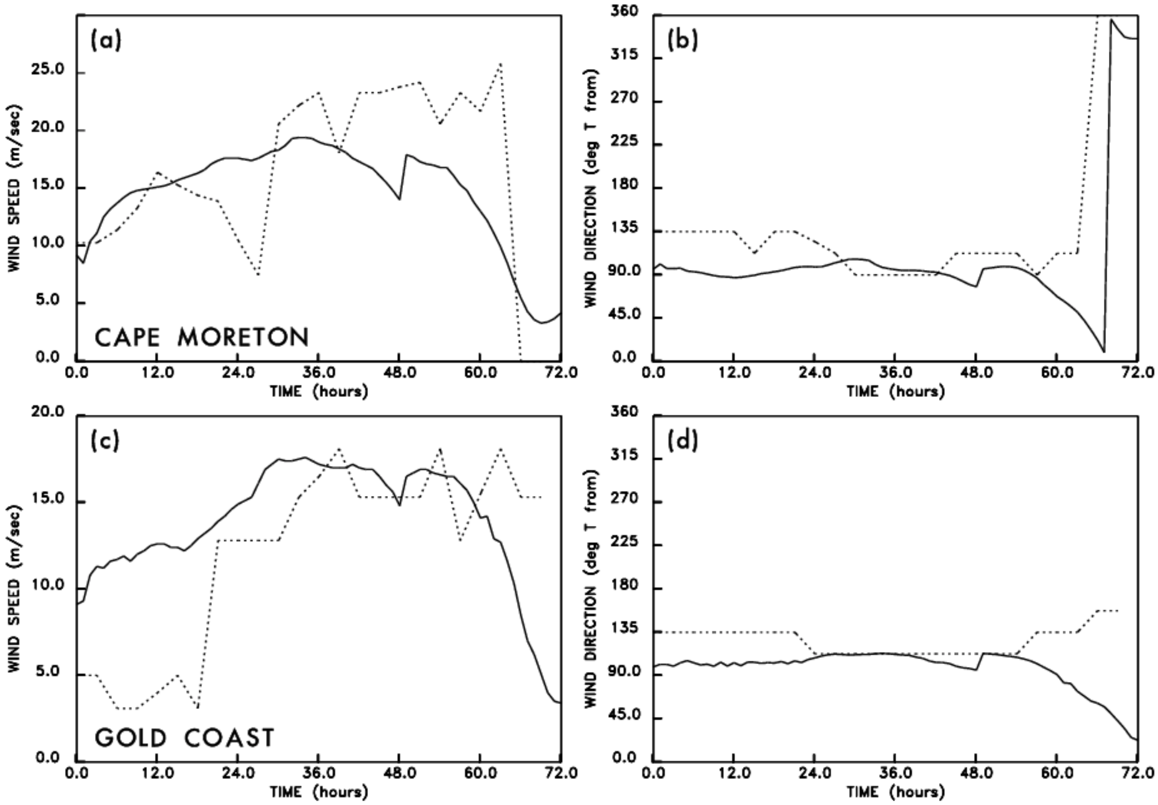

Figure 16: Modelled and observed wind speed and direction at Cape Moreton (a) and (b), and the Gold Coast (c) and (d).

6.1.2 Tidal Model Results

Prior to running GCOM2D with atmospheric forcing, a tides-only simulation was carried out over the coarse resolution model domain to ascertain how well tidal variations are represented. These are compared with the tides predicted using the known tidal phases and amplitudes. Results for the three-day interval commencing 0000 UTC 23 April 1989 are shown for the Brisbane Bar and the Seaway in Figure 17. Also shown are the observed sea levels indicating the degree of meteorological influence on the coastal ocean during this period. Tides are predominantly semi-diurnal in this region and the tidal range at Brisbane Bar is approximately 0.6 m greater than that at the Seaway. This may be due to the hydraulic resistance created by the channel islands at the southern end of the Bay.

Model simulations conducted using GCOM2D underestimate the higher high tide by approximately 0.1 m at Brisbane Bar. However values at low tide and lower high tide are well captured. At the Gold Coast Seaway, much closer agreement is seen between the modelled and predicted tides at high tide whereas the lower high tide is overestimated by GCOM2D by about 0.1 m. There is a slight phase error between the modelled and predicted tides with the modelled tide leading the predicted tide by up to an hour.

The agreement in Figure 17 is a good result considering that GCOM2D derives its tidal boundary conditions from a global tidal model (the Grenoble model) with a resolution of half a degree. For GCOM2D to translate the open ocean tidal conditions from the global tidal model into Moreton Bay, the Broadwater and the Gold Coast with such small errors suggests that GCOM2D is modelling the tidal dynamics in the shallow regions extremely accurately. The global tidal model itself has much larger errors in the shallow coastal regions.

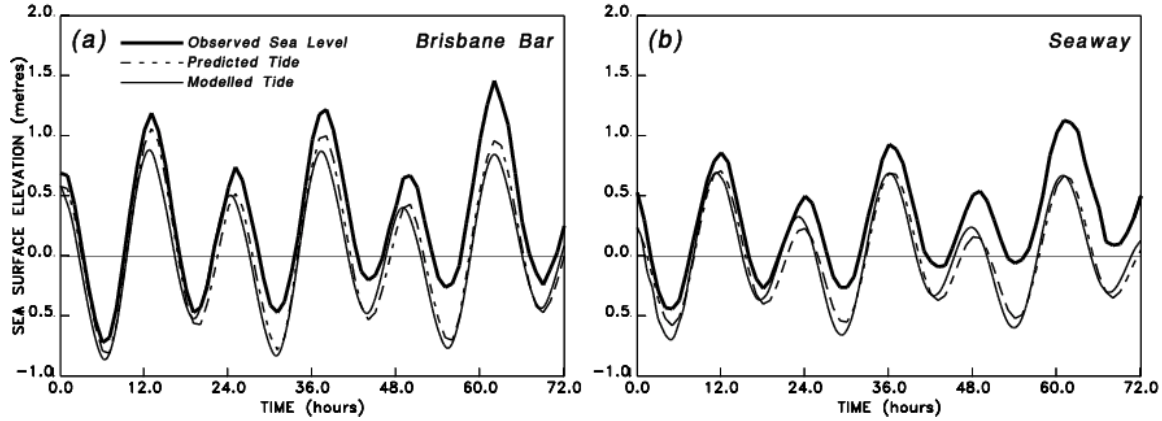

Figure 17: Predicted and modelled tides at (a) Brisbane Bar and (b) the Gold Coast Seaway. For comparison, the observed sea levels (also containing contributions from storm surge and wave setup) are shown. The simulation commences at 0000 UTC 23 April 1989.

6.1.3 Wave Model Results

The incorporation of radiation stress forcing in GCOM2D requires the simulation of wave heights, directions and periods. In this section, we examine briefly the results from a 72-hour simulation of the wave conditions for the April 1989 event using the third generation wave model WAM. Figure 18 shows the simulated wave heights, directions and periods at 0000 UTC 25 April 1989. Wave heights exceed 6 m over a region immediately to the east of Moreton Island extending southwards to the Gold Coast and are directed onshore. The wave periods in this region are in excess of 8 seconds. For this event, significant wave heights of up to 6.5 m were recorded off Moreton Island with wave periods of 10.62 s. (Allan and Callaghan, 2000).

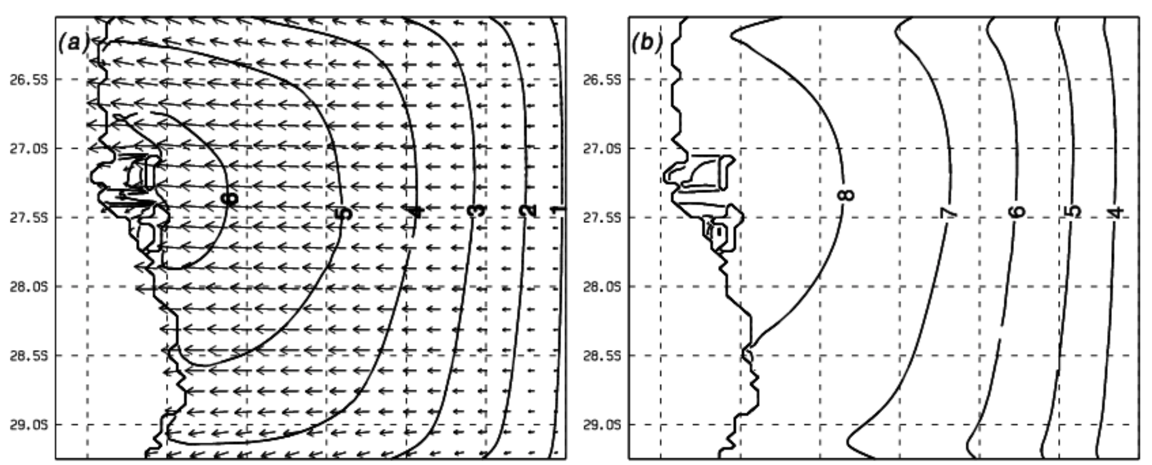

Figure 18: (a) Wave height (in metres) and direction and (b) wave period (in seconds) at 0000 UTC 25 April 1989 as simulated by the WAM model.

6.1.4 Storm Surge and Wave Setup Results

Three fine mesh model simulations were conducted. The first incorporated tidal forcing only, the second had tides and wind forcing and the third also contained wave radiation stresses. Time series for the third simulation at the Seaway and the northern and southern arm of the Coomera River are shown in Figure 19 along with the observed sea level at the Seaway. Note that only the last 24 hours of the simulation, when the highest sea levels occurred, are shown. Comparing the modelled and observed sea levels at the Seaway reveals that a slight phase difference is evident and is consistent with that seen on the coarse resolution tides-only simulation. The modelled sea-level heights are also underestimated by about 0.1 m. The underestimation of sea levels by the model, particularly in the last 12 hours, may be due to an underestimation of the wind strength along with a shift to northeasterlies in the atmospheric model simulation that was not seen in the observations.

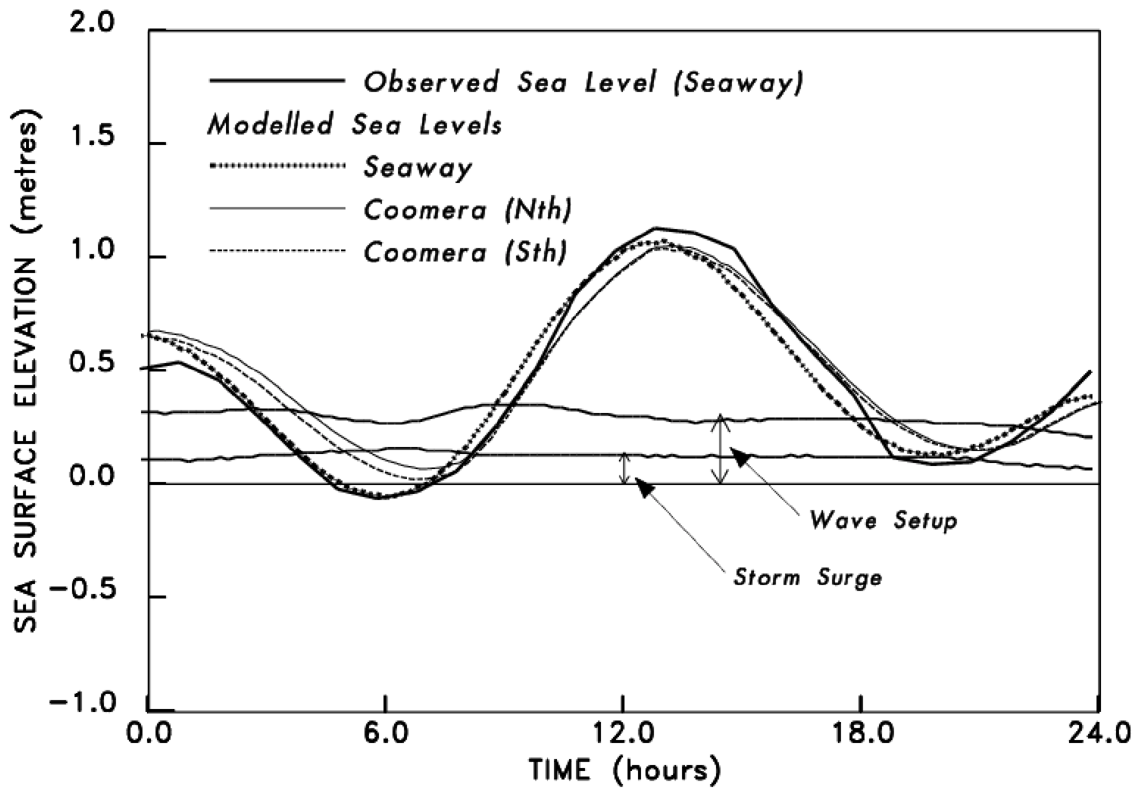

Figure 19: Modelled and observed sea levels at the locations indicated. The storm surge and wave setup components of the total sea-level signal at the Seaway are also shown. The time series commences at 0000 UTC 25 April 1989.

The sea levels at the northern and southern arms of the Coomera River show lower sea-level peaks occurring approximately one hour later. This phase delay is consistent with the observed tidal signals at the Seaway and the southern arm of the Coomera (Paradise Point).

To investigate the relative contribution from wave setup, the sea-level results from the tides and surge simulation at the Seaway were subtracted from the full simulation that also included wave radiation stresses. The resulting residual is shown in Figure 19 and indicates that the contribution from wave setup was relatively uniform during the 24-hour period and accounted for approximately 0.25 - 0.30 m of the total sea level. The contribution due to the storm surge was obtained by subtracting the sea levels due to tides-only from the tides plus surge simulation. The result indicates that there was a contribution to the sea levels due to the storm surge of between 0.10 - 0.15 m. This finding is consistent with the results of a study into the relative contributions of storm surge and wave setup to the sea levels recorded along the NSW coast during severe east coast low events (McInnes and Hubbert, 2000).

Figure 20a shows the current vectors at 1200 UTC on April 1989 corresponding to high tide. A northerly current exceeding 0.5 m s^{-1} is evident along the east coast while in southern Moreton Bay, it is southerly. Flow at Jumpinpin and the Seaway is into the Broadwater. Currents shown six hours later (Figure 20b), indicate that the tides have turned and flow is to the north in Moreton Bay. Flow at Jumpinpin and the Seaway are directed towards the east. Height contour charts (not shown) indicate that there was only minimal inundation of low lying land within the Broadwater.

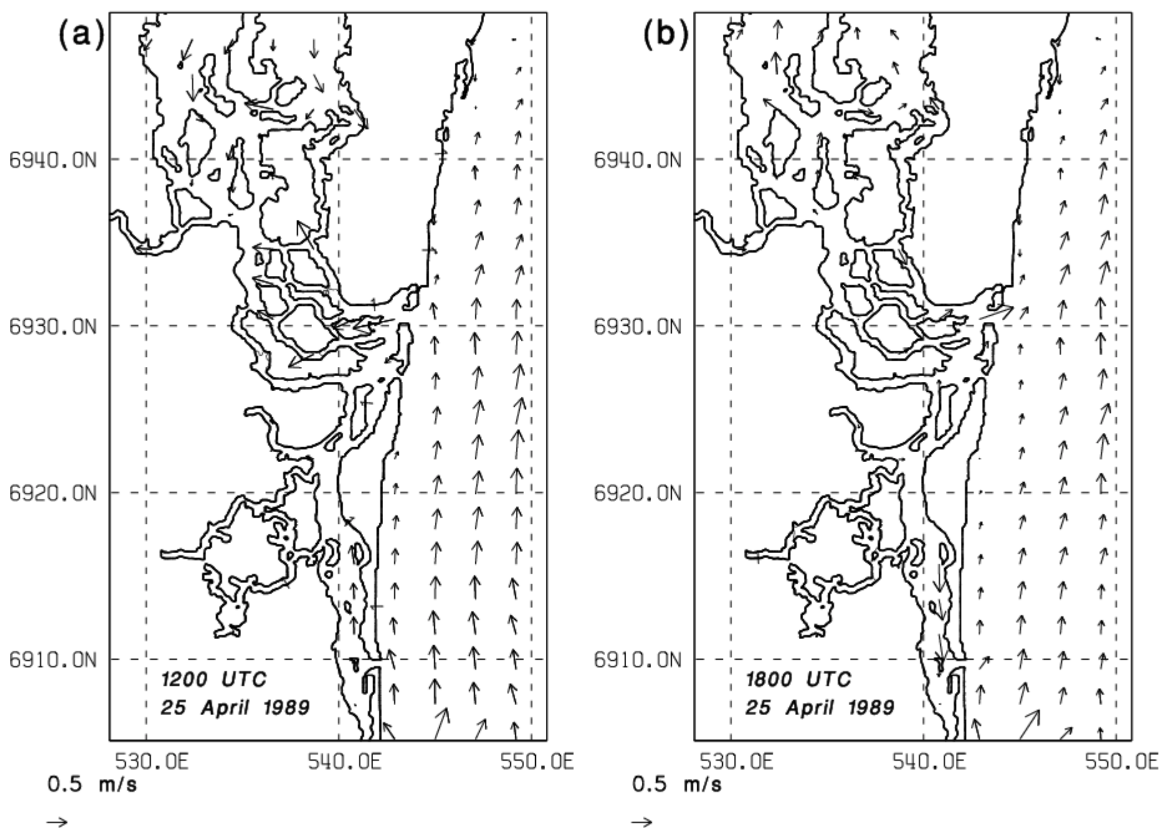

Figure 20: Modelled currents at (a) 1200 UTC 25 April and (b) 1800 UTC 25 April.

6.2 Case 2: Tropical Cyclone Wanda

Tropical cyclone Wanda was responsible for major flooding from Brisbane to the Gold Coast. Severe beach erosion also occurred along the south Queensland coast. Freshwater runoff was a major factor in the flooding within the Broadwater. As a result, the fresh water flux (derived previously from various hydraulic modelling studies) is also incorporated into GCOM2D. The flow hydrographs are shown in Figure 21 and indicate that the peak combined discharge from the five rivers was around 11000 m^3 s. The locations at which these fluxes are applied is indicated in Figure 4b (note that the Coomera flux is divided across the two branches). Bathymetry at the Seaway has been modified to reflect the 1974 conditions and a sensitivity experiment utilizing present day bathymetry is also conducted.

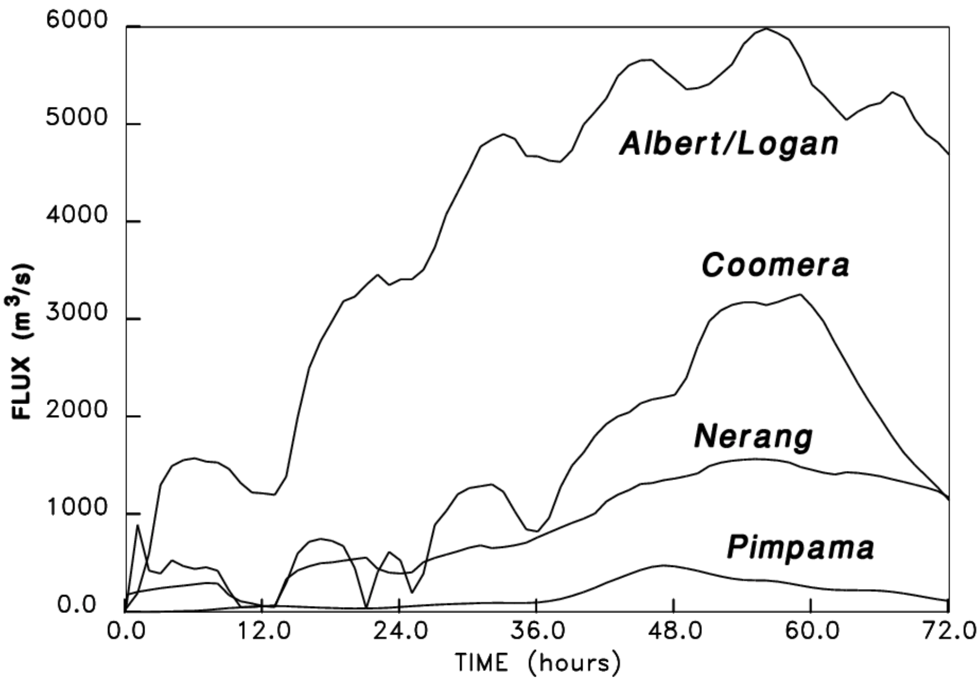

Figure 21: Volume of water flow along the major rivers that flow into the Broadwater during the 1974 flood.

6.2.1 Atmospheric Model Results

At 2300 UTC 23 January 1974 (Figure 22a) a tropical depression embedded in a strong monsoon trough approached the Queensland coast to the north of Fraser Island. By 1100 UTC 24 January 1974, the depression had intensified to 1000 hPa as it made landfall producing strong winds to the south of the low centre (Figure 22b). A simulation of the event commencing at 1200 UTC 23 January 1974 was performed using the RAMS atmospheric model. At 12 hours into the model simulation (Figure 22c), the trough of low pressure has deepened from 1010 hPa at the initialization time to 1006 hPa. This is slightly weaker than the observed low of 1004 hPa although the location of the low is well captured. At 1100 UTC 24 January, the model has captured the broad monsoon trough but has failed to capture the development of the low pressure system.

The observed winds associated with the low pressure system in Figure 22a are from east to south-east and have strengths between 10 and 18 m s^{-1}. The strongest winds along the Queensland coastline lie between the northern tip of Fraser Island and Moreton Bay. The model also predicts the strongest winds to occur in this region with wind speeds between 12 and 16 m s^{-1} (Figure 22c). Both the model and analyzed winds are much weaker inland with speeds less than 10 m s^{-1}. The region with winds greater than 12 m s^{-1} has moved towards the coast since the initial time. By 1100 UTC 24 January wind speeds along the Gold Coast are between 12-17 m s^{-1}, having strengthened from 10 m s^{-1} observed 12 hours earlier. The model also moves the region of strong winds to the south with a broad region of winds in excess of 12 m s^{-1} occurring between the Sunshine Coast and northern NSW. However due to the failure of the model to simulate the development of the closed low, the winds along the Gold Coast are from the east-northeast rather than the east-southeast or east as in the observations.

At later times, manual analyses were not available for comparison with the model simulation. However, comparison of measured wind speed and direction at Brisbane airport (Figure 23) with model simulated winds indicates that the modelled winds increasingly gained a northeasterly component whereas the observations indicated winds uniformly from the east or east-southeast up to about 0000 UTC 26 January. The greatest impact of the increasing northerly component in the modelled winds would be a reduction in the storm surge along the open coast compared with that generated by winds directed onshore or from the south.

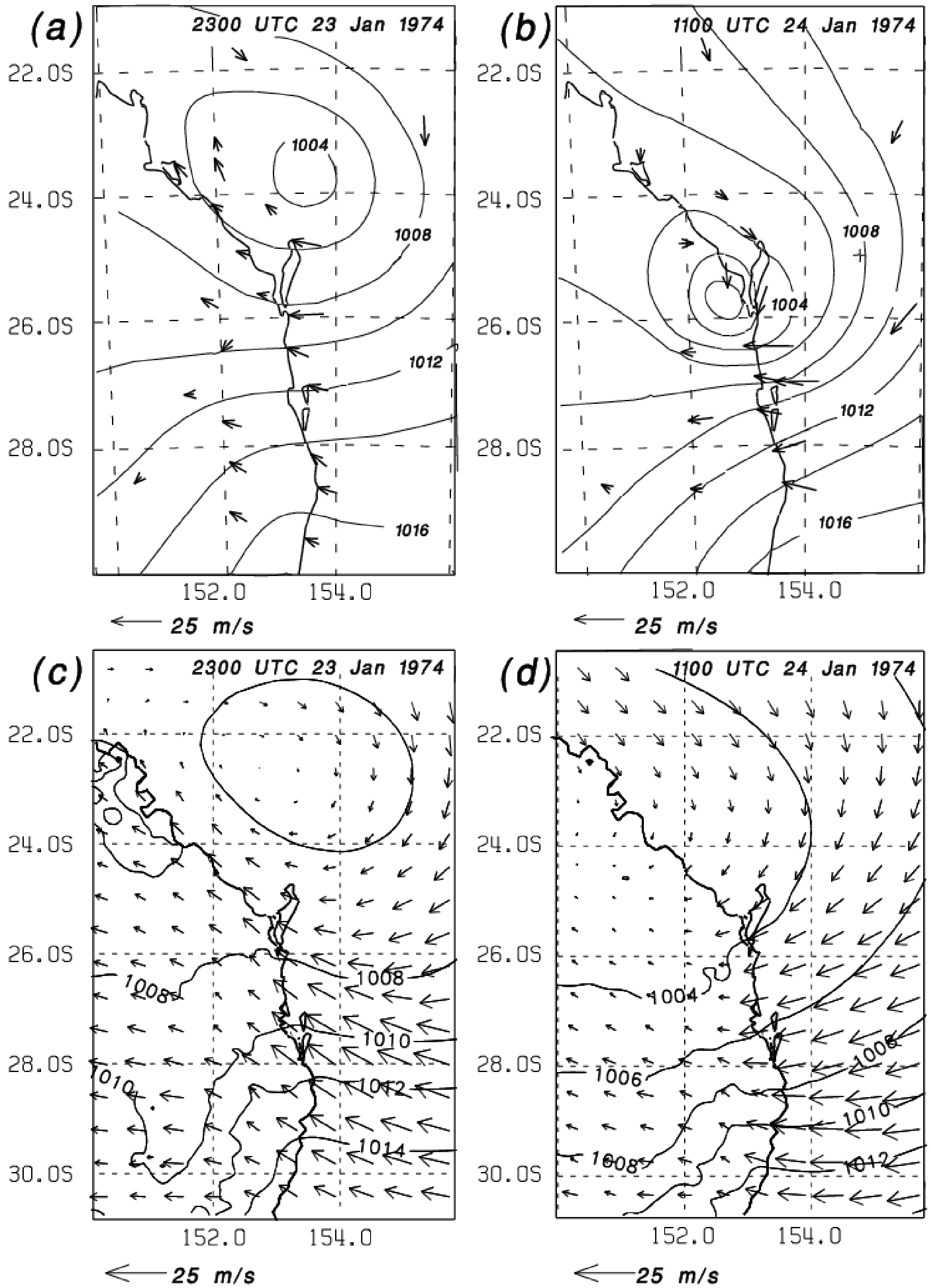

Figure 22: (a)-(b) Manual analyses of mean sea level pressure at the times indicated with observed surface wind vectors also shown. (c)-(d) RAMS model simulations of mean sea level pressure and 10-m wind vectors at the corresponding times. (Note that only a subset of the RAMS model grid corresponding to the area covered by the analyses is shown).

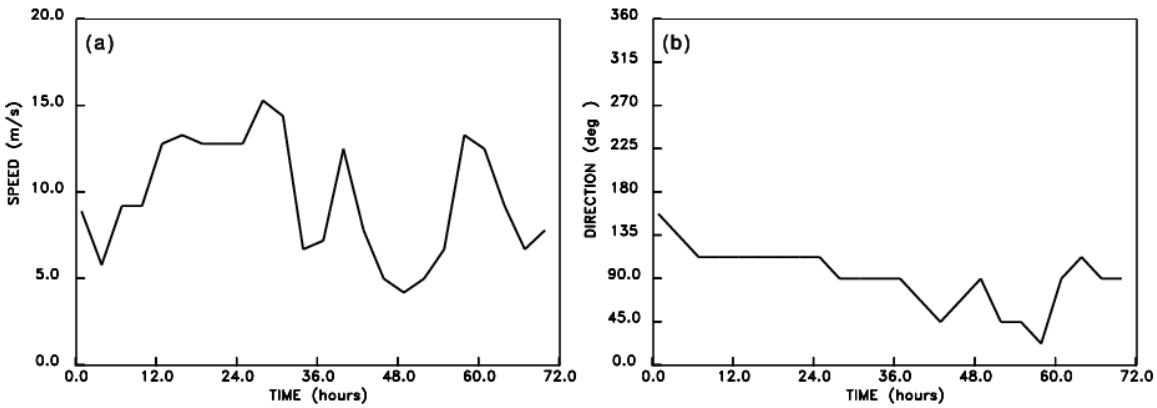

Figure 23: Measured (a) wind speed and (b) direction for the time period commencing 0000 UTC 24 January 1974 at Brisbane airport.

6.2.2 Ocean Response

Three simulations of GCOM2D were carried out over 72 hours commencing 0000 UTC 24 January 1974 using bathymetry modified in the vicinity of the Seaway to approximate 1974 conditions. The first was a tides-only simulation, the second incorporated tides, storm surge and wave setup (referred to here as the saltwater simulation) and the third was a full simulation including freshwater runoff from the key river systems flowing into the Broadwater as well as the saltwater contribution.

Figure 24a compares the water levels from the full simulation of GCOM2D with those measured in the southern Broadwater. Modelled water levels show reasonable agreement with observations although low tides and lower high tides are slightly overestimated. The higher high tide at 24 hours into the simulation is underestimated by about 0.2 m. Examination of the relative contributions to the total water level are also examined. The contribution due to storm surge and wave setup, calculated by subtracting the time series of the tides-only simulation from the saltwater simulation, is shown in Figure 24a. The maximum contribution of about 0.4 m occurs at around 12 hours into the simulation and decreases thereafter. A further breakdown of this time series to determine the storm surge component (not shown) indicates that the storm surge reaches a maximum of 0.1 m at about 12 hours and decreases to zero by 24 hours. The lack of a storm surge signal from 24 hours onwards may be a reflection of the northerly bias in the modelled winds in the simulation at around this time compared with observations as discussed previously, and may account for the underestimation of the total sea levels at around this time. The wave setup may also be underestimated slightly.

Observed wind speeds and directions shown in Figure 23 suggest that the most favourable conditions for wave setup and storm surge along the Gold Coast are in the 36 hours up to 1200 UTC 25 January and indeed this is borne out in Figure 24a. The flux hydrographs shown in Figure 21 indicate that the latter 36 hours are when the greatest contribution to Broadwater sea levels due to freshwater influx may be expected. The modelled freshwater contribution, calculated by subtracting the time series of the saltwater simulation from the full simulation, is also shown in Figure 24a and indicates that indeed the largest freshwater contribution occurs in the latter 36 hours. It is noteworthy that the freshwater time series exhibits a tidal-like oscillation that is 180° out-of-phase with the tide. This is presumably a response to the greater hydraulic resistance that occurs at high tide and causes the water to back up and flow onto adjacent floodplain areas.

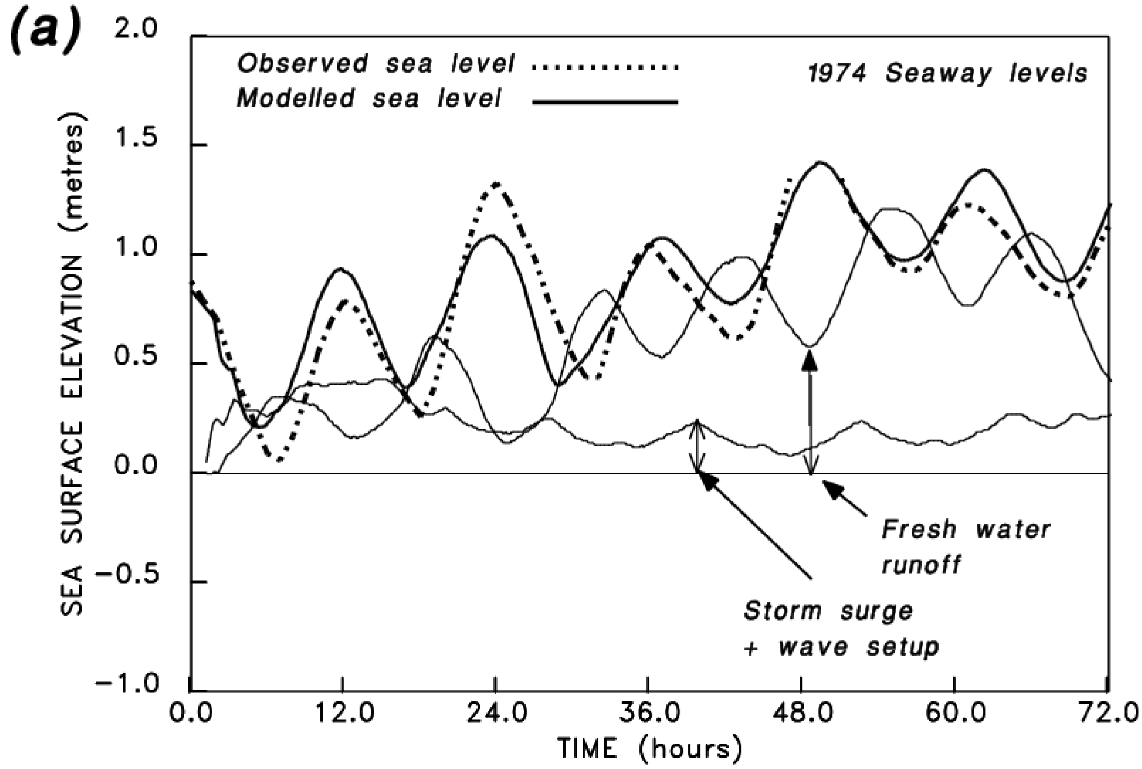

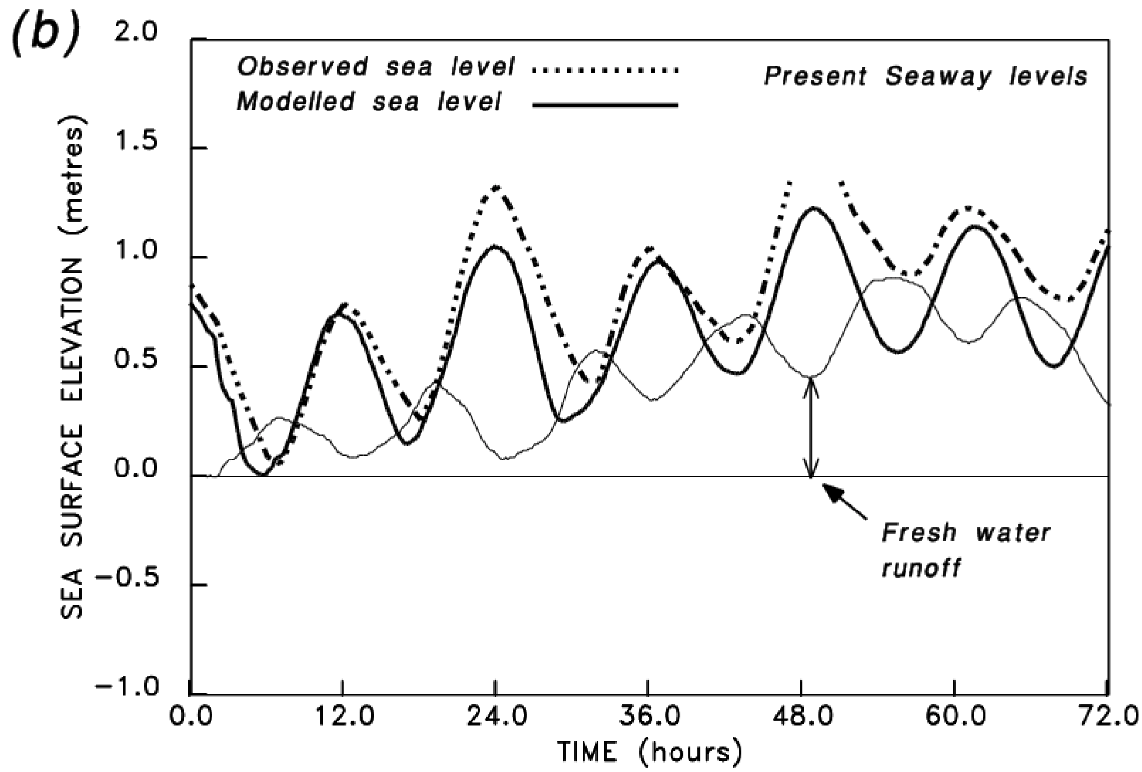

Figure 24: (a) Observed sea levels at Southport and corresponding modelled sea levels using 1974 bathymetry at the Seaway (note, there is missing data at around 48 hours). Also shown are contributions due to freshwater runoff and saltwater (storm surge and wave setup). (b) as for (a) except using present day bathymetry.

Figure 24b shows the water levels attained in a model simulation that utilizes present day bathymetry at the Seaway. Water levels are around 0.3 m lower at high tide and 0.4 m lower at low tide. This relative difference may reflect more effective drainage occurring at low tide as a result of the deeper Seaway.

Figure 25a shows the current vectors at 1800 UTC on 25 January corresponding to low tide in the present day bathymetry simulation. A southerly current of around 0.5 m s^{-1} is evident along the east coast while in southern Moreton Bay, flow is northward. At Jumpinpin and the Seaway, easterly flow of about 1.0 m s^{-1} is evident. Currents shown six hours later (Figure 25b), just prior to high tide, indicate dramatically reduced inflow in southern Moreton Bay, and weaker easterly flow at Jumpinpin and the Seaway. Clearly the high water levels within the Broadwater are driving currents in these regions that counter the tidal currents. The extent of the flooded land is also shown in Figure 25 and covers an area of approximately 120 square km.

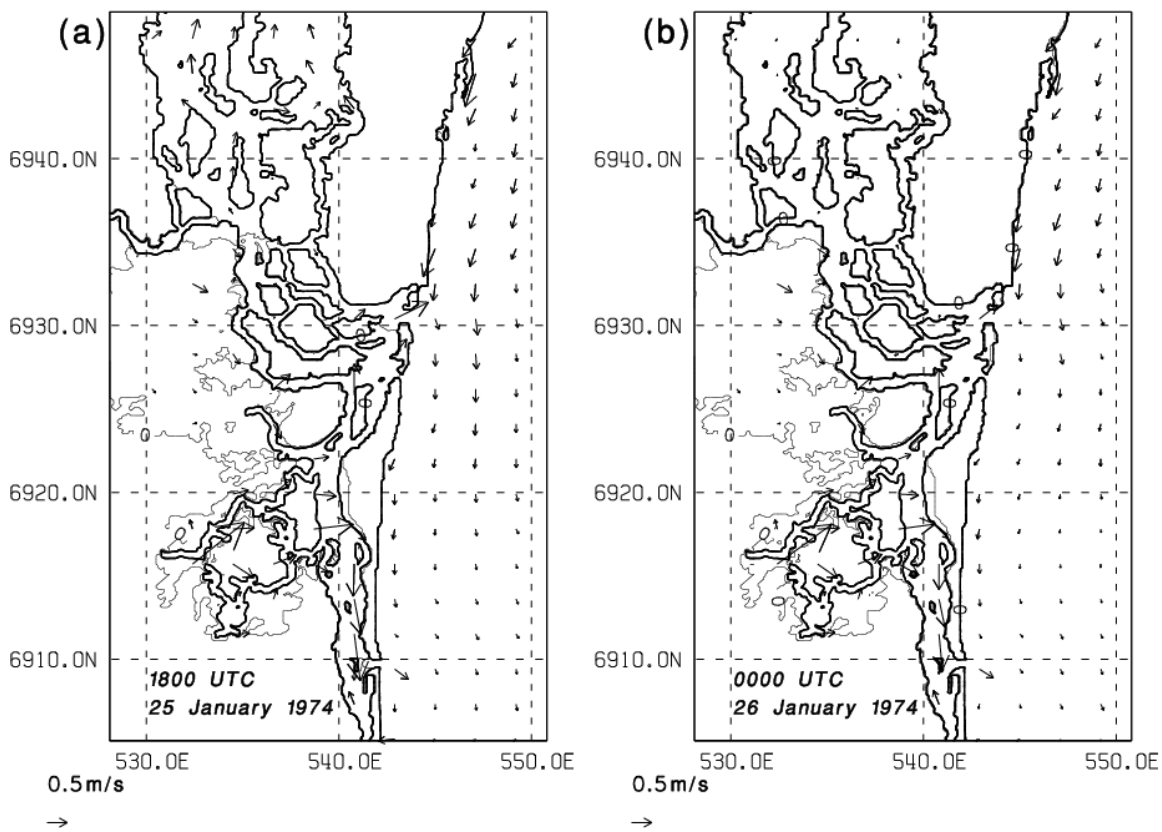

Figure 25: Modelled currents at (a) 1800 UTC 25 January and (b) 0000 UTC 26 January. The contour defining the flooded land area is also shown.

A comparison of modelled water levels in the Broadwater and on the open coast at high tide is made in the latter half of the simulation when the freshwater flux is at a maximum. This indicates that the Broadwater levels are around 0.5 m higher than water levels on the open coast. This is the opposite tendency to the saltwater events in which the storm tide level on the open coast is typically about 0.1 m higher that the Broadwater levels.

7. Discussion and Conclusions

This study has seen the use of a sophisticated modelling system to evaluate the return periods of storm tides within the Broadwater of the Gold Coast. It is the first study of its type to focus on this complex region. The coastal ocean and inundation model GCOM2D, capable of modelling tides, storm surges and overland flow was further developed to simulate the effects of wave setup. Wave conditions required as input were simulated using a third generation wave model.

A methodology was developed for the evaluation of storm tide statistics that integrated the contributions to extreme sea levels produced by two predominant classes of meteorological phenomena that impact on this region- tropical cyclones and east coast lows. The storm tides due to tropical cyclones were evaluated using a Monte-Carlo approach. A statistical representation of the key cyclone characteristics was developed from the historical cyclone record from which cyclones could be randomly selected for storm tide simulations. This approach effectively generates a synthetic sea-level record from which extreme events can be analysed statistically.

Return periods for east coast low events were evaluated by simulating a large number of actual events that have occurred within the last 20 years and applying extreme value analysis to the resulting storm tide values. While generally less robust than the methodology for tropical cyclones due to the relatively small number of events simulated, it was considered appropriate since these events were found to contribute to the low end of the spectrum for storm tide events. The two sets of results were combined using joint probability analysis. Results yielded sea levels for given return periods in the Broadwater that were lower than values previously adopted for planning purposes. The lower values may be due to the implicit calculation of wave setup in the present study leading to lower value of total sea level than the more conservative approach often adopted of adding a uniform value of wave setup to previously evaluated storm surge results.

Detailed simulations were carried out of two cases: the April 1989 east coast low and tropical cyclone Wanda (responsible for the 1974 floods). The modelling system was able to reproduce the April event with a high degree of accuracy. Simulations suggested that the greatest contribution to sea levels during the east coast low event was due to the wave setup rather than the storm surge.

To simulate the 1974 flood event, data from flow hydrographs for the five main river systems flowing into the Broadwater were also incorporated as boundary conditions to GCOM2D along with the tidal, wind and wave forcing. In addition, the bathymetry in the vicinity of the Seaway was modified to reflect the shallower channel that existed at that time. The model simulations of the water levels were reasonably well captured although some discrepancies were noted.

The storm surge and wave setup made their largest contribution to the water levels during the first half of the simulation. It is likely that the storm surge and, to a lesser extent, the wave setup were underestimated due to errors in the modelled wind field. Nesting conditions for the atmospheric model were based on NCEP analyses, which are created by assimilating available meteorological observations into a forecast model to produce more detailed meteorological analyses. Limited open ocean data available in 1974 would lead to less accurate analyses over ocean regions. This conclusion is further supported by the fact that the wind directions in the atmospheric model showed a bias to the northeast. Other factors that could provide a minor contribution to differences between the model and observations in the present study may include omission of runoff from minor tributaries and rainfall directly over the catchment.

During the latter half of the simulation, freshwater runoff was the main contributor to the sea levels in the Broadwater. This particular event highlights the fact that rainfall has the capacity to considerably worsen the impact of extreme storm tide events in this region. As a consequence of this, future efforts to determine the risk of severe floods in the Broadwater should incorporate freshwater runoff in combination with wave setup and storm surge to be inclusive of all the major physical processes. A simulation of the 1974 flood event with present day bathymetry produced sea levels that were between about 0.3 and 0.4 m lower than those attained with the 1974 bathymetry.

Due to the relatively long planning horizon implied by the return periods, it would also be of value to integrate the likely impact of climate change on the climatology of cyclones and east coast lows, as well as the expected changes to extreme rainfall runoff. Increases in sea level due to the enhanced Greenhouse effect have been estimated for the Gold Coast to be between 3 and 58 cm with a central estimate of 18 cm by 2050 (Walsh et al., 1998). These projections increase the risk of extreme events occurring. For example, at the Seaway an 18-cm sea-level rise transforms the 1-in-100 year event into a 1-in-50 year event.

References

Allan, M. and J. Callaghan, 2000: Extreme wave conditions for the south Queensland coastal region. Environment Technical Report 32, Environmental Protection Agency.

Battjes, J.A. and J.P.F.M. Janssen, 1978: Energy loss and setup due to breaking in random waves. Proc. 16th Int. Conf. on Coastal Eng., Hamburg, 569-587.

Blain, Bremner and Williams Pty Ltd, 1985: Storm tide Statistics – Surfers Paradise Region. Report prepared for the Beach Protection Authority, Queensland. January, 1985. 15 pp.

Harper, B.A., 1999: Storm tide threat in Queensland: History, prediction and relative risks. Department of Environment and Heritage. Technical report no. 10. 24 pp.

Harper, B.A., R.J. Sobey and K.P. Stark, 1977: Numerical simulation of tropical cyclone storm surge along the Queensland coast, Part X – Gold Coast. Department of Civil and Systems Engineering, James Cook University, Townsville. 15 pp.

Holland, G.J., 1980: An analytical model of the wind and pressure profiles in hurricanes. *Mon. Wea. Rev.*, **108**, 1212-1218.

Holmes, J.D. and W.W. Moriarty. 1999: Application of the Generalised Pareto Distribution to wind engineering. *J. Wind Engineering and Industrial Aerodynamics*. **83**, 1-10.

Hubbert, G.D., G.J. Holland, L.M. Leslie and M.J. Manton, 1991: A real-time system for forecasting tropical cyclone storm surges. *Weather and Forecasting*, **6**, 86-97.

Hubbert, G.D., L.M. Leslie and M.J. Manton, 1990: A storm surge model for the Australian region. *Quart. J. Roy. Met. Soc*., **116,** 1005-1020.

Hubbert, G.D. and K.L. McInnes, 1999a: A storm surge inundation model for coastal planning and impact studies. *J. Coastal Research*. **15,** 168-185.

Hubbert, G.D. and K.L. McInnes, 1999b: *Modelling storm surges and coastal ocean flooding.* In: 'Modelling coastal sea processes', Ed. B.J. Noye, World Scientific Publishing Co., 159-187.

Mastenbroek, C., G. Burgers, and P.A.E.M. Janssen, 1993: The dynamical coupling of a wave model and a storm surge model through the atmospheric boundary layer. *J. Phys. Oceanog.* **23**. 1856-1866.

McInnes, K.L. and Hubbert, G.D. 2000: The impact of eastern Australian cut-off lows on coastal sea levels. *Meteorological Applications* (to appear).

Mei, C. C., 1983: "The applied dynamics of ocean surface waves". Wiley Interscience. New York. 740 pp.

Tremback, C., G. Tripoli, R. Arritt, W. R. Cotton, and R. A. Pielke, 1986: The Regional Atmospheric Modelling System. Int. Conf. Development and Applications of Computer Techniques to Environmental Studies, Los Angeles, U.S.A. 601-607

Walsh, K.J.E., D.R. Jackett, T.J. McDougall, and A.B. Pittock, 1998: Global warming and sea level rise on the gold coast. Report prepared for the Gold Coast City Council, April 1998.

The WAMDI Group, 1988: The WAM Model – A Third Generation Ocean Wave Prediction Model. *J. Phys. Oceanog.* 18, 1775-1810.

WMO, 1988. World Meteorological Guide to Wave Analysis and Forecasting. WMO No. 702.

Yeh, G.-T., and F.-K. Chou, 1979: Moving boundary numerical surge model. *J. Waterw. Port Coastal and Ocean Div*., **105**, 247-263.

Acknowledgements

GEMS would like to acknowledge the information and time provided by the following persons and organisations that have made a significant voluntary contribution to this study:

Mr Haydn Betts, Gold Coast City Council
Lawson and Treloar (Brisbane)
Mr Geoff Callaghan, Brisbane Severe Weather Office of the Bureau of Meteorology
The Bureau of Meteorology Head Office, Melbourne
Dr Tom Beer, CSIRO Atmospheric Research
Queensland Department of Transport.

Appendix 1: The Wave Breaking Algorithm

Deepwater wave heights calculated by the WAM model are adjusted for breaking in GCOM2D as follows. The probability of a wave exceeding height H_1 is governed by the Rayleigh distribution so that

$$\Pr(H > H_1) = \exp\left\{-2\left(\frac{H_1}{H_{s0}}\right)^2\right\}, \tag{1.1}$$

where H_{s0} is the incident significant wave height (the average of the highest one third of waves) (WMO, 1988). Within the surf zone, wave heights decrease in proportion to the local depth so that

$$H = \gamma \, d , \tag{1.2}$$

where γ typically varies from 0.6 to 1.0 and is taken here to be 0.7 and *d* is the water depth. Tests carried out where H_{s0} = 5.0 m and γ was set to 0.6 and 0.8 respectively yielded wave setups that varied from minus to plus 10% of the result obtained with γ = 0.7. From (1), the fraction of waves exceeding $H_{\max}$ is

$$Fr(H > H_{\max}) = \exp\left\{-2\left(\frac{H_{\max}}{H_{s0}}\right)^2\right\}. \tag{1.3}$$

We need to calculate the significant wave heights H_s of the remaining waves assuming that the fraction of waves above $H_{\max}$ have been dissipated through breaking. We let $H_{\min}$ denote the lowest wave height in the group containing the highest one third of waves and so the fraction of unbroken waves for a given H_{s0} is

$$Fr(H > H_{\min}) = \frac{2}{3}\left[1 - Fr(H > H_{\max})\right] = \frac{2}{3}\left[1 - \exp\left\{-2\left(\frac{H_{\max}}{H_s}\right)^2\right\}\right]. \tag{1.4}$$

Since

$$Fr(H > H_{\min}) = \exp\left\{-2\left(\frac{H_{\max}}{H_s}\right)^2\right\}, \tag{1.5}$$

we can solve for $H_{\min}$. Once $H_{\min}$ is known, H_s can be calculated over the range $H_{\min}$ to $H_{\max}$ by breaking the wave range into equal increments and weighting the average according to the distribution of wave heights given by (1).

The appropriately modified wave heights are then applied at each time step to determine the radiation stresses according to their shallow water approximations, (Mei, 1983)

$$
\begin{aligned}
S_{xx} &\cong \frac{E}{2}\left(2\cos^2\theta + 1\right) \\
S_{yy} &\cong \frac{E}{2}\left(2\sin^2\theta + 1\right) \\
S_{xy} &= S_{yx} \cong E\sin\theta\cos\theta
\end{aligned}
\tag{1.6}
$$

where θ is the wave angle with respect to the x-axis and the wave energy, E, is given by

$$
E = \frac{1}{8}\rho g H_{rms}^2 \tag{1.7}
$$

where H_{rms} is the rms wave height. The radiation stresses are then introduced into GCOM2D through the horizontal momentum equations. The resulting shoreward decrease in wave height and hence radiation stress due to wave breaking produces a net increase in water level.

Appendix 2: The Parametric Cyclone Model

The parametric cyclone model is based on Holland (1980) and its application to storm surge modelling is described in Hubbert et al. (1991). The pressure P (hPa) at radius r is derived as follows,

$$P = P_c + (P_n - P_c) e^{-(r_m/r)^b} \tag{2.1}$$

where P_c is the central pressure, P_n is the environmental pressure (the climatological mean for the region and month), r_m is the radius of maximum winds and b provides a scaling on the profile shape. The parameter b is empirically defined by

$$b = 1.5 + (980 - P_c)/120 \tag{2.2}$$

with P_c in hPa. The symmetric, gradient-level azimuthal wind component is estimated by

$$v = \left[b \left(\frac{r_m}{r} \right)^b \frac{(P_n - P_c)}{\rho} e^{-(r_m/r)^b} - \frac{r^2 f^2}{4} \right]^{\frac{1}{2}} - \frac{rf}{2} \tag{2.3}$$

where ρ is the air density and f is the Coriolis parameter.

A first-order asymmetry is included by adding the cyclone translation to the symmetric field and rotating the field so that the maximum wind is 70^o to the left (right in the Northern Hemisphere) of the direction of cyclone motion. The radial wind field is constructed by rotating the flow to a constant inflow angle of 25^o outside the radius of maximum winds.

Appendix 3: Generalised Pareto Distribution

In this study the Generalized Pareto Distribution (GPD) has been used to fit both extremes of tropical cyclone pressure and storm surge levels. Although the Type I Extreme Value Distribution is more commonly used in engineering applications, it is actually a special case of the Extreme Value Distribution (GEV)

$$Fv(V) = \exp\left\{ -\left(1 - \frac{k(V-a)}{b}\right)^{\frac{1}{k}} \right\}, \tag{3.1}$$

where *V* is the variate, *k* is a shape factor and *a* and *b* are the location and scale parameters respectively. When $k < 0$ the GEV is known as a Type II Extreme Value Distribution, when $k > 0$ it becomes a Type III Extreme Value Distribution (a form of the Weibell Distribution). In the limit as $k \rightarrow 0$ Equation A1 becomes

$$Fv(V) = \exp\left\{ -\exp\left(-\frac{(V-a)}{b}\right) \right\}, \tag{3.2}$$

the well-known Type I Extreme Value Distribution (Gumbel Distribution).

Since the Type I and Type II distributions predict unlimited values for increasing return period they may be artificially conservative. On the other hand, the Type III distribution has the advantage that it curves in such a way as to approach a limiting value – this characteristic lends the distribution to application in the current study.

Holmes and Moriarty (1999) have shown how the Type III distribution can be applied in wind engineering applications. The GPD for a variate, y, takes the form

$$Fy(y) = \left\{ 1 - \left(1 - \frac{ky}{\sigma}\right)^{\frac{1}{k}} \right\}, \tag{3.3}$$

where σ is scale factor and k is a shape factor. The case $k < 0$ is the usual Pareto Distribution.

An estimate of the return period value V_R of the underlying variable *V* can be obtained from

$$V_R = U_0 + \sigma\left(\frac{1-(\lambda R)^{-k}}{k} \right), \tag{3.4}$$

where λ is the number of events that meet the specified threshold over a given time period. Holmes and Moriarty describe a convenient method for determining the scale and shape parameters σ and *k*.

The method has been shown to be valuable across several studies. At lower return periods (order 100 years) application of the Type I and Type III return period estimates have generally been shown to produce only small differences. However, at larger return periods application of the Type III distribution is shown to be less conservative and in accord with natural occurring physical limits (such as for cyclone intensity).